Mullard Technical Communications

JULY 1971
Volume 12 Number 111

Contents

2 Design of power transformers having ferrite cores
27 Pulse-modulator thyristor BTW35 as a radar magnetron driver
30 Solid aluminium electrolytic capacitors, 121-series

Mullard Limited Mullard House Torrington Place London WC1E 7HD

Mullard Technical Communications

VOLUME 12 NUMBER 111 July 1971

Design of power transformers having ferrite cores *E. C. Snelling* 2

Pulse-modulator thyristor BTW35 as a radar magnetron driver *M. Keohane* 27

Solid aluminium electrolytic capacitors, 121-series *B. Goudswaard* 30

This journal records developments in the application of electronics in science, industry, and the home. It contains information on the properties and performance of solid-state devices, valves and tubes, and associated components and assemblies. The practical circuits given are designed to provide the best working conditions and performance for the devices used. The design principles may be used (so far as device ratings allow) for adaptation to meet particular requirements. Current data should be consulted before any circuit is considered for production. Mullard Limited can normally supply only those devices or assemblies listed in the Company's current catalogues. Availability in quantity should be confirmed.

All information is published in good faith, but because of the wide variety of situations in which this information may be used, we cannot accept any responsibility for loss or damage resulting from unsatisfactory performance. Publication of this information does not imply any authority or licence for the utilisation of any patented feature.

Four issues are published each year and issued free of charge to equipment designers, research organisations, laboratories, libraries, educational establishments, and consultants. Requests for addition to the mailing list must be made on the official stationery of the establishment concerned.

Technical enquiries should be addressed to the Editor. Abstracts or references should mention both source and authors. Requests for republication or translation should be made to the Editor in writing.

'Mullard' is the trade mark of Mullard Limited and is registered in most of the principal countries of the world.

Editor: F. A. Sowan Assistant Editor: E. G. Evans

Central Technical Services,

Mullard Limited, Mullard House, Torrington Place, London, WC1E 7HD

Telephone: 01-580 6633 Telex: 264341

©Mullard Limited, 1971

Made and Printed in England by
WIGHTMAN AND COMPANY LIMITED, 1/3 BRIXTON ROAD, LONDON, SW9 6DS

Design of power transformers having ferrite cores

E. C. SNELLING
Mullard Research Laboratories

621.344.21.026.441/4 : 621.318.124

The design of power transformers with ferrite cores is considered in detail in this article. The electrical design is treated fully for both low frequencies and high frequencies, and procedures for core selection and winding design are emphasised. In particular, methods of calculation and minimization of eddy current losses in the windings are given. The calculation of heat transfer and temperature rise is also fully covered.

INTRODUCTION

The transformers considered in this article are those which transmit such relatively large powers that the design is mainly limited by saturation or the heating of the core or windings. Although the treatment is related to the use of ferrite cores much of it is quite general in its application. Current transformers and high energy inductors are not specifically included but a large proportion of the treatment is relevant to the design of these devices also.

Power transformers may be required to transmit at a single frequency, such as in a power distribution network, or over a narrow band of frequencies, as in the output of an ultrasonic generator, or over a wide band of frequencies, as in an aerial matching unit.

Single frequency and narrow band transformers sometimes have a regulation specification which may override the limitations arising from saturation or heating. The regulation depends not only on the winding losses but also on the leakage inductance; indeed the design of such transformers may be determined mainly by the winding resistance and leakage inductance.

Wideband power transformers will normally have to meet a return loss requirement over a given frequency band as well as having acceptable power losses. Therefore the design of such transformers necessitates a combination of the design procedures for wideband telecommunication transformers and those for single frequency power transformers. Normally such a transformer would be initially designed as a single frequency power transformer at the lower frequency of the transmission band and then the design would be checked, again as a single frequency transformer, at the upper frequency of the band. Having achieved a satisfactory design as a power transformer, the wideband transmission requirements, such as return loss, would then be considered and the design would be developed accordingly.

It will be seen later that as the frequency to be transmitted becomes lower then, for a given temperature rise, the flux density at which the core may operate becomes higher, until a frequency is reached below which the design is limited by the saturation of the core. For a silicon iron core the maximum working flux density is typically 1·5T ($1{\cdot}5 \times 10^4$Gs) and the saturation value is typically 2T (2×10^4Gs). From published data for ferrites the corresponding figures would be typically 0·35 and 0·5T (3500 and 5000Gs) respectively. Therefore at the lower power frequencies, for example 50Hz and 400Hz, the transformer steels have a distinct advantage over ferrites. However, at higher frequencies, where loss considerations dominate the design, the ferrite cores find a wide variety of applications. Typical examples are a 2kW, 30kHz output transformer to supply an ultrasonic power transducer and a 5kW antenna matching transformer operating over a frequency band from 2 to 30MHz. As suggested above, the design procedure will depend on which factors predominate in the particular problem and this information must be deduced at the commencement of the design.

Common to most power transformer designs is the heat transfer problem and this is considered first. Then there is a general discussion of the electrical design of transformers operating at frequencies that are not so high that the eddy current losses in the windings are significant. This is followed by a more detailed study of three types of design, namely the regulation limited, the saturation limited and the core loss limited design. Finally the problems of the higher frequency power transformer are considered.

HEAT TRANSFER AND TEMPERATURE RISE

General

A part of the power applied to the primary of a transformer is dissipated in the form of heat due to losses in the windings, in the core, and in the dielectric materials that insulate the winding. The latter loss is usually negligible but may become significant in high voltage transformers. These losses cause a rise in temperature, the equilibrium temperature being reached when the heat lost balances the heat produced in the transformer. Since the production of heat per unit volume will in general vary from one part of the transformer to another and because the thermal conductivities involved are finite, the temperature, and therefore the rate of heat transfer, will in general vary from place to place on the surface of the transformer.

From the engineering point of view the temperature is important mainly because of its effects, usually deleterious, on the properties of the materials composing the transformer, for example increase of copper resistance, increase of core losses, reduction of the saturation flux density of the core material and degradation of the insulating materials. Since these effects concern the interior of the transformer it is the interior temperature that is important and this will be higher than the surface temperature by an amount depending on the thermal conductivities of the transformer materials and the distribution of the heat sources.

Sometimes the designer is more concerned with the heat dissipation than the temperature rise, because, for example, the efficiency of the transformer may be important or its contribution to the ambient temperature inside an equipment may be a design criterion. At equilibrium, the calculation of the rate of heat dissipation usually presents no problems of heat transfer because it equals the total power loss. The present discussion is therefore concerned mainly with the temperatures attained by the transformer.

As indicated above, the surface temperature is a function of the rate of production of heat, that is, power loss, and the heat dissipating properties of the transformer assembly. The heat will in general be transferred to the surroundings by means of conduction, convection and by radiation, and each of these processes may be natural or may be artificially aided. The way in which the total heat transfer is proportioned between these means of dissipation will vary widely from one design to another.

Enough has been said to illustrate the complexity presented by a proper analysis of the heat transfer problem. However since great accuracy is not normally required, simplifying assumptions may be made. In the extreme case these lead to the rule of thumb that a heat loss of about 300μW per square millimetre of surface (0·2W.in^{-2}) is a reasonable design figure. The design of a highly rated power transformer usually requires a more reliable guide. Accordingly data will now be given that will enable most transformer temperature problems to be solved with reasonable accuracy. Since the transformers under discussion are not large by power engineering standards they attain equilibrium temperature in a relatively short time and it is this equilibrium temperature that is of main concern. The transient heating and cooling problem arises when the operation is intermittent or when the transformer is so large that the thermal time constant is too long for convenient measurement of the equilibrium temperature. The transient problem is dealt with in most text books on power transformers.

A transformer is usually cooled mainly by convection (forced or natural) assisted by radiation. The amount of cooling by conduction is significant only if special means are adopted to make it so; for example, some transformers are equipped with special heat conductors and heat sinks so that conduction is the principal means of cooling. However the majority of transformers are not designed in this way so attention will be devoted mainly to the other two types of cooling.

A transformer may be operated in contact with surrounding air or it may be contained in an oil filled vessel. In either design the transfer of heat depends ultimately on the radiation and convection from the surface in contact with the air (incidental conduction and the possibility of water cooling being ignored). The convection may be natural, or forced air cooling may be provided. The treatment below starts with the cooling of a body in air.

If the transformer is contained in an oil filled vessel then the heat must be transferred from the transformer surface to the volume of oil before being dissipated to the surrounding air. This process is next considered. Finally attention is given to the passage of heat from the interior of the transformer to its surface. Applying these calculations in the above order enables the complete heat transfer problem to be solved in principle. In practice the procedure is reasonably reliable unless some factor is present which either invalidates the assumptions, for example, significant conduction, or complicates the calculation, for example an unusual winding arrangement.

Radiation

This is taken first not because it is necessarily the most important means of cooling but because it does not depend on the ambient air conditions.

The rate of dissipation of heat from a surface follows from the Stefan-Boltzmann law and is given by:

$$P_{rad} = 5{\cdot}67 \times 10^{-8} E(T_s^4 - T_o^4) \ \ \mu W.mm^{-2} \quad \ldots(1)$$

where E is the emissivity of the surface

T_s is the surface temperature of the transformer in K

and T_o is the temperature of the surrounding objects in K

The values of emissivity for a number of surfaces are given in Table 1.

In subsequent calculations involving radiation, T_o will be assumed to be 300 K (27°C) and E will be taken as 0·95.

TABLE 1
The emissivities of various surfaces (after King, Ref. 1)

Surface	Emissivity E
Polished aluminium and brass	0·05
Clean, smooth iron and steel	0·2
Polished silver	0·025
Oxidised aluminium	0·1–0·2
Oxidised brass	0·25–0·6
Oxidised iron and steel	0·6–0·9
Metallic paint	0·5
Non-metallic solids such as porcelain, glass, paper and non-metallic paints of any colour	0·9–0·95

This article is based on Chapter 9 of 'Soft Ferrites—Properties and Applications', Iliffe, London (1969) by the same author. Permission to reproduce this material is acknowledged.
© E. C. Snelling.

These data have been used to calculate the broken curve in Fig. 1; this expresses the relation given in Eq. 1 and may be used to find the heat lost by radiation in most practical situations. Radiation loss under other conditions may be readily obtained from the above equation.

Convection

Convection is the removal of heat by the passage of a fluid over a surface.

The fluid in close proximity to the surface may be regarded as a stagnant film transmitting heat by conduction to the main body of the fluid which due to its movement may be regarded as a constant temperature heat sink. There is, of course, a gradual transition between the stagnant film and the main body of the fluid. The rate of heat dissipation depends on the properties of the fluid and the difference in temperature between the surface and the fluid; it does not depend on the fine texture or the colour of the surface.

In free convection the movement of the fluid arises from its reduced density when heated. It gathers heat as it rises over the heated surface and subsequently loses it to the surrounding fluid or containing vessel, becomes more dense as it cools and descends, perhaps to recycle past the heated surface indefinitely. Clearly the rate of heat transfer per unit area of surface will be influenced by the geometry of the surface; for example, a vertical surface will lose heat by free convection at a rate different to that from a horizontal surface.

In forced convection the fluid is passed over the surface at a velocity determined only by the performance of the pump or blower. Thus the rate of cooling is less dependent on the geometry of the surface but obviously depends on the fluid velocity.

Free convection of air

Two formulae are quoted from the literature. For a long horizontal cylinder in air at atmospheric pressure the following formula is derived from one quoted by King (Ref. 2)

$$P_{conv} = 6{\cdot}3\frac{\theta^{1\cdot25}}{d^{0\cdot25}} \quad \mu W.mm^{-2} \qquad \ldots(2)$$

where P_{conv} is the rate of heat transfer by convection,

θ is the difference in temperature in deg.C between the surface and the air,

d is the diameter of the cylinder in mm.

When the diameter exceeds 150 to 200mm (6 to 8in) the rate of heat transfer per unit area tends to become independent of the diameter, and the body may be treated as a number of large plane surfaces. A formula is given below for the heat transfer from a large vertical surface. Before considering this however it should be mentioned that Eq. 2 may be extended to apply to all bodies having dimensions which are small enough to affect the convection per unit area, that is, linear dimensions of less than about 300mm (12in). This is done by giving d an effective value depending on the horizontal dimension and the vertical dimension of the given body, d_{hor} and d_{vert} respectively (Ref. 3).

Then
$$\frac{1}{d} = \frac{1}{d_{hor}} + \frac{1}{d_{vert}} \qquad \ldots(3)$$

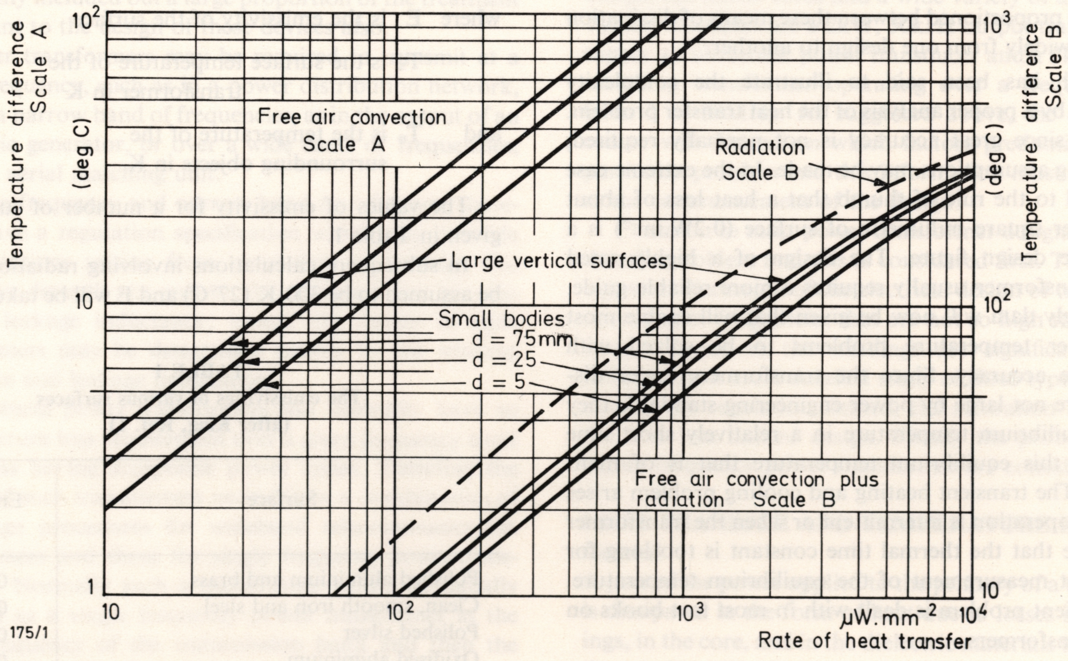

Fig. 1—Heat transfer by free air convection and radiation. The temperature difference between the surface and the surrounding air as a function of the rate of heat transfer for: large vertical surfaces (heights > 0·6m or 24in), and small bodies having various values of d in mm where d = diameter for long horizontal cylinders or $d = d_{hor}d_{vert}/(d_{hor}+d_{vert})$ for more compact bodies in which the horizontal length d_{hor} becomes comparable with the vertical height, d_{vert}. For small spheres d = radius. The L.H. group of curves is for free air convection, the broken curve is for radiation assuming a surface emissivity of 0·95 and an ambient temperature of 27°C, and the R.H. group is for the sum of the convection and radiation. Based on data given by King (Ref. 2) and Montsinger (Ref. 4)

Thus for a sphere 1/d = 2/diameter, therefore d equals the radius of the sphere. This method is applicable to most power transformers used with electronic apparatus.

For vertical surfaces having heights greater than 600mm (24in) Montsinger (Ref. 4) gives a formula which may be stated as follows

$$P_{conv} = 2{\cdot}17\theta^{1\cdot25} \quad \mu W.mm^{-2} \qquad \ldots(4)$$

(θ is defined in Eq. 2)

From the upper side of a plane horizontal surface the rate of heat loss will be 15 to 25% more than for a vertical surface, and for a similar downward facing surface the rate of heat loss will be less and will decrease as the surface becomes larger; a reduction of 33% relative to the vertical surface is quoted by King.

If the air pressure is n atmospheres then both of the heat transfer expressions, that is, the R.H.S. of Eq. 2 and 4, must be multiplied by $\sqrt{n}$, thus natural convection at high altitudes is much less effective.

Fig. 1 shows the surface temperature rise above ambient as a function of the rate of heat transfer at normal atmospheric pressure. The left hand group of curves are for free convection cooling of horizontal cylinders or small bodies in accordance with Eq. 2 and for large vertical surfaces in accordance with Eq. 4. The broken curve is for radiation cooling under the conditions mentioned in connection with Eq. 1. The right hand group of curves are for free convection plus radiation and, neglecting conduction losses, represent the equilibrium temperatures of typical bodies cooling under normal atmospheric conditions.

For free convection at normal atmospheric pressures the thickness of the stagnant film referred to above is about 2 to 3mm. This must be remembered when considering clearances. If the space between the surface of the winding and the outside leg of a shell type core is less than 10mm then the convection cooling from these surfaces will be less than the calculated value. If the spacing approaches 3mm it may be assumed that no cooling by free convection will occur in that space and the areas concerned must be disregarded in calculating the total cooling surface of the transformer. Similarly any surface which clears an adjacent obstruction by less than about 5mm will lose relatively little heat by free convection. If the transformer or its case is fitted with cooling fins these should be at least 12mm (0·5in) apart if they are to contribute to cooling by free convection. In fact the effective area of such fins may be estimated by assuming that their surfaces (but not their exposed edges) and the surfaces from which they project are covered by a 6mm thickness of conductive material. The derived surface, including the (now thickened) exposed edges of the fins may be used to calculate the effective area.

Forced convection in air

For air flowing over a plane surface King (Ref. 5) gives a formula from which the following expressions may be obtained

$$P_{conv} = (4{\cdot}54+4{\cdot}1v)\theta \quad \mu W.mm^{-2} \qquad \ldots(5)$$

where v is the velocity of the air stream at a distance of about 25mm from the surface, in $m.s^{-1}$, and

θ is the temperature difference between the surface and the air in deg C

or

$$P_{conv} = (4{\cdot}54+1{\cdot}25v)\theta \quad \mu W.mm^{-2}$$

where the symbols are as before except that v is in $ft.s^{-1}$.

Fig. 2 shows the relative surface temperature as a function of the rate of heat transfer due to forced air

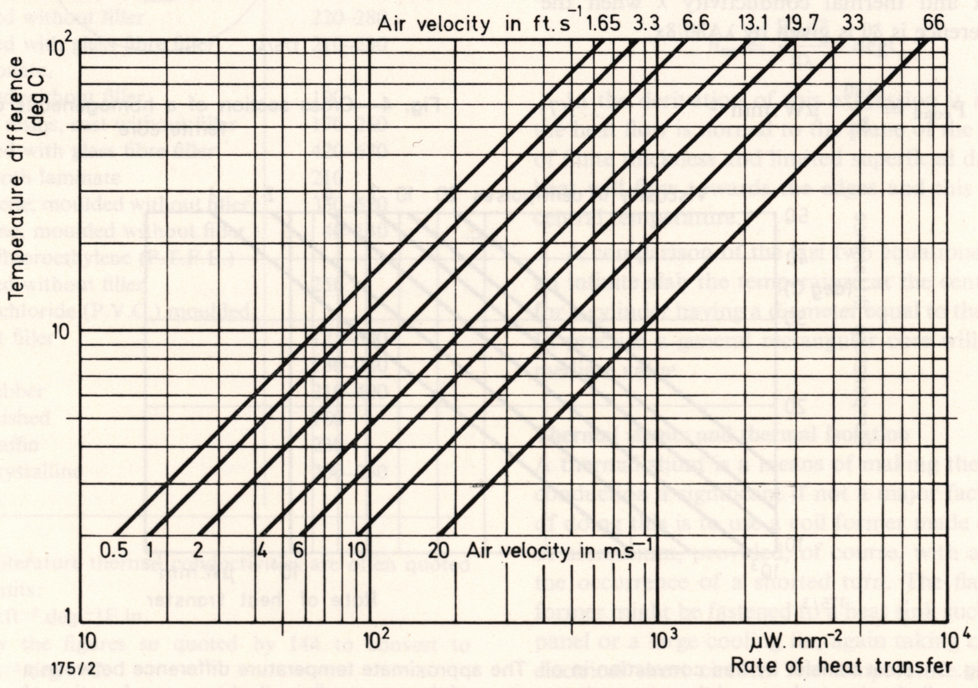

Fig. 2—Heat transfer by forced air convection. The temperature difference between the surface and the surrounding air as a function of the rate of heat transfer for various air velocities. These data apply to air flow parallel to a smooth surface. If the surface is rough the transfer may be up to 40% greater; if the air meets the surface at an oblique angle the transfer is somewhat less. Based on data quoted by King (Ref. 5)

cooling. The amount of radiation cooling is usually relatively small but if it is significant it may be added from the data given in Fig. 1.

Free convection in oil

In an oil immersed transformer the heat is normally transferred from the transformer surface to the walls of the containing vessel by free convection. The rate of heat transfer per unit area depends on the viscosity and other properties of the oil and also on the temperature difference, θ, between the transformer surface and the main body of the oil. In practice the main body of the oil may be assumed to be at a temperature that is not much higher than the walls of the containing vessel when these are cooled by air convection. King (Ref. 6) quotes results obtained by Montsinger and Metrovick, and suggests that these results may be approximately represented by

$$P_{conv} = \frac{112\theta^{1 \cdot 25}}{\nu^{0 \cdot 4}} \ \mu W.mm^{-2} \qquad \ldots(6)$$

where ν is the oil viscosity in centipoises measured at a temperature that is a mean between that of the dissipating surface and the bulk of the oil.

This expression is shown graphically in Fig. 3.

The remarks made concerning the effect of the stagnant layer between the surface and the convection currents apply here also except that the effective skin thickness is about 1 to 1·5mm. Thus if convection cooling is to be assisted by providing vertical ducts in the core or winding these should have least dimensions of not less than 3mm. If this limitation is observed then the surface area of the duct may be added to the total cooling area.

Conduction

The rate of heat flow perpendicular to a lamina of area A, thickness δx and thermal conductivity λ when the temperature difference is δθ is given by λAδθ/δx, or

$$P_{cond} = \frac{\lambda\delta\theta}{\delta x} \quad \mu W.mm^{-2} \qquad \ldots(7)$$

where P_{cond} is the rate of heat transfer by conduction per unit area
δx is in mm
δθ is in degC
λ is in $\mu W.mm^{-1}.deg^{-1}C$.

This may conveniently be regarded as the ‘ohms law’ of heat flow by conduction:

$$P_{cond} = \frac{\delta\theta}{R_T} \quad \mu W.mm^{-2} \qquad \ldots(8)$$

where R_T is the thermal resistance (δx/λ) and has the units: $degC.mm^2.\mu W^{-1}$.

Given the thermal resistance of a layer through which a uniform perpendicular heat transfer is occurring, the temperature difference across the layer may be readily calculated. Where the heat flow is divergent, P_{cond} is not constant across the thickness and the temperature drop must be obtained by integration.

The thermal conductivities of some commonly used transformer materials are given in Table 2.

Pursuing the electrical analogy, a complex arrangement of heat sources and heat transfer paths may be represented by an equivalent electrical circuit of current sources and resistances.

Before leaving conduction, it will be convenient to consider the heat transfer in a homogeneous ferrite core. Fig. 4 shows the cross-section of a cylindrical core of radius r and axial length l. The power converted to heat in unit volume of the ferrite, P_m, is assumed to be uniform and therefore at thermal equilibrium the heat passing through an elementary surface of radius x is

$$P_m \pi x^2 l \ \ W.$$

The heat flow per unit area is

$$\frac{P_m \pi x^2 l}{2\pi x l} = \frac{P_m x}{2} = P_{cond}.$$

Therefore from Eq. 7

$$d\theta = \frac{P_m x}{2} \ \frac{dx}{\lambda}$$

Integrating from x = 0 to x = r, the temperature difference between the centre and the surface is

$$\theta_{cs} = \frac{P_m r^2}{4\lambda} = \frac{P_m d^2}{16\lambda} \ degC \ . \qquad \ldots(9)$$

If λ is in $\mu W.mm^{-1}.deg^{-1}C$ and the diameter d is in mm then P_m is in $\mu W.mm^{-3}$ or $mW.cm^{-3}$.

For normal sizes of ferrite cores operating at typical frequencies and flux densities this conductive temperature drop is not large. Where it is large then Eq. 9 becomes invalid since both P_m and λ are functions of temperature and this should be allowed for in the integration.

For cores with cross-sections approximating to a square, Eq. 9 may be used with reasonable accuracy if the effective diameter d is taken as the diameter of the circle having the same area, A, as the rectangular core, that is $d = (4A/\pi)^{\frac{1}{2}}$.

A similar treatment of ferrite cores having cross-sections with rectangular dimensions b × d where b ≫ d, that is, relatively thin slabs of ferrite, yields a temperature difference between the central plane and the parallel surfaces given by

$$\theta_{cs} = \frac{P_m d^2}{8\lambda} \quad degC \qquad \ldots(10)$$

In the derivation of this expression it is assumed that the heat flow is normal to the plane of the slab; for a slab of finite thickness and limited superficial dimensions some heat will flow towards the edges and this will reduce the central temperature.

A comparison of the last two equations shows that for an infinite slab the temperature at the centre is twice that for a cylinder having a diameter equal to the slab thickness. In practice a general rectangular core will have an intermediate value.

Thermal shunts and thermal isolation

A thermal shunt is a means of making the cooling due to conduction a significant if not a major factor. One means of doing this is to use a coil former made of a metal such as aluminium, provided, of course, with a slit to prevent the occurrence of a shorted turn. The flange of the coil former might be fastened to a heat sink such as a chassis, a panel or a large cooling fin, again taking care to avoid an electrical short circuit. The temperature of the heat sink would depend on the heat flowing into it from the thermal shunt and on its rate of cooling due to convection, etc. This may be readily obtained from the heat transfer graphs

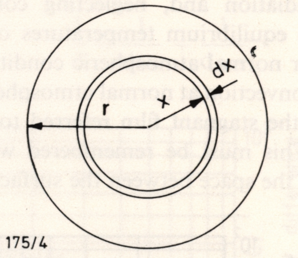

Fig. 4—Cross section of a homogeneous cylindrical ferrite core

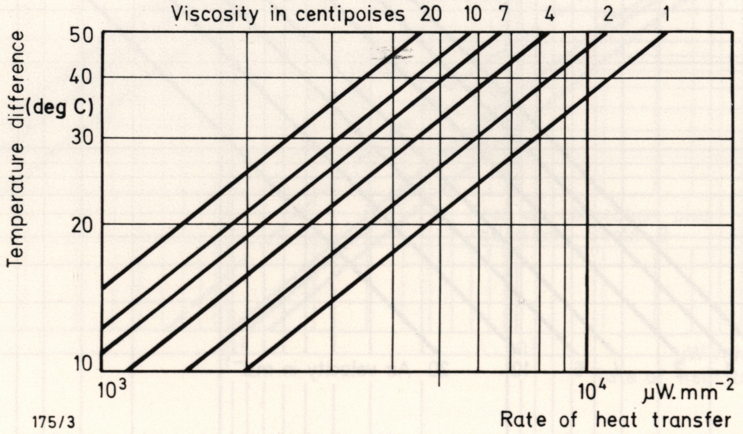

Fig. 3—Heat transfer by free convection in oil. The approximate temperature difference between a large dissipating surface and the average temperature of the surrounding oil, shown as a function of the rate of heat transfer with the oil viscosity as a parameter. The viscosity is the value corresponding to a temperature that is a mean between that of the dissipating surface and the bulk of the oil. Based on data quoted by King (Ref. 6)

TABLE 2

Thermal conductivities of some materials commonly used in power transformers

Material	Thermal Conductivity, λ in $\mu W.mm^{-1}.deg^{-1}C$. at 20°C
Metals	
Aluminium, 90% pure	220×10^3
Brass	111×10^3
Copper	385×10^3
Lead	38×10^3
Silver	410×10^3
Steel	43×10^3
Insulating materials	
Alumina ceramics	$(10–30)\times10^3$
Cotton cloth, varnished	160–220
Bitumen	420–700
Epoxy resin, cast without filler	170–210
Epoxy resin, cast with silica filler	400–850
Ferrite	3500–4300
Glass	720–1200
Glass bonded mica	380–600
Mica	400–600
Paper, dry	50–140
Paper board, varnished	250
Phenol formaldehyde (Bakelite etc)	
moulded without filler	125–250
moulded with wood flour filler	170–350
paper laminate	240–260
fabric laminate	320
Polyamide resin (Nylon etc)	
moulded without filler	220–280
moulded with glass fibre filler	210–280
Polycarbonate, moulded without filler	190
Polyester resins, cast without filler	170–260
moulded with glass fibre filler	420–670
glass cloth laminate	210
Polyethylene, moulded without filler	330–520
Polystyrene, moulded without filler	40–140
Polytetrafluoroethylene (P.T.F.E.)	
moulded without filler	250
Polyvinylchloride (P.V.C.) moulded without filler	125–300
Rubber	130–280
Silicon rubber	210–400
Silk, varnished	160
Wax, paraffin	230
microcrystalline	200–250

Note. In the literature thermal conductivities are often quoted in the units:
$Btu.h^{-1}.ft^{-2}.deg^{-1}F.in.$
Multiply the figures so quoted by 144 to convert to $\mu W.mm^{-1}.deg^{-1}C$.

shown earlier in this section. Usually the heat sink temperature will be near that of the equipment ambient so a very effective heat transfer path is provided.

An alternative or additional means of reducing winding temperatures is to isolate the heat coming from the core and prevent it from entering the windings. This may be done, for example, by making a sufficiently large gap between core and coil former so that all the core heat is carried away by direct convection.

Further ways of dealing with the heat transfer problem are to be found in the literature. Sufficient has been included here to enable the designer to obtain a reasonably accurate estimate of the equilibrium temperatures within a proposed transformer.

GENERAL ELECTRICAL DESIGN CONSIDERATIONS

The basic relation is the e.m.f. equation

$$E = \frac{\omega \hat{B}_e A_e N}{\sqrt{2}} \quad V \qquad \ldots(11)$$

where $\hat{B}_e$ is the peak value of the effective flux density in teslas

A_e is the effective* core cross-sectional area in m^2

and N is the number of turns.

The freedom of design implicit in this equation is usually restricted by other considerations; the more important of these will be considered later. For the moment it is useful to discuss qualitatively the e.m.f. equation in relation to a given source voltage U_1 ($\approx$ E in practice) and a given core.

Since the core losses rise with frequency and flux density, the flux density at high frequencies is usually limited to relatively low values by the permissible core loss. At high frequencies the necessary low flux densities may be obtained with relatively few turns. If the number of turns required to obtain the permissible flux density is too small to provide sufficient shunt impedance then N must be suitably increased; this will reduce the flux density and both the reactive and core loss components of the magnetizing current will be reduced.

For a given voltage and core, $\hat{B}N \propto 1/f$. The core loss expressed in watts is approximately proportional to $f\hat{B}_e^n$ where n lies between 1·9 and 2·9 approximately. Thus for a given core loss $\hat{B}_e \propto 1/f^{1/n}$. It follows that as the frequency is decreased, both the flux density and the number of turns will increase if the core loss is maintained at a specified value. Under these conditions the design is core loss limited. In such a design it may be advantageous to obtain a certain ratio between core loss and copper loss in order to achieve optimum performance with respect to efficiency or volume, etc.

At lower frequencies the flux density will approach the saturation value and will become limited. Below this frequency the design is saturation limited. At progressively lower frequencies the core loss decreases and the winding loss rises because N must now rise in inverse proportion to f in order to keep $\hat{B}_e$ constant. The total power loss, or temperature rise, is still the factor limiting the throughput.

At even lower frequencies the winding resistance or leakage inductance will become large enough to result in an unacceptable regulation. Below this frequency the design is regulation limited and the temperature rise ceases to be a restriction.

The shunt inductance has been mentioned above. This is often a major parameter in transformer design. If it is too low, the magnetizing current will be too great; in a wideband transformer this will cause excessive attenuation or insufficient return loss at the lower end of the transmission band. Except for tuned transformers, the shunt inductance is usually required to be greater than a specified value. However, excessive values may be accompanied by a leakage inductance or a winding resistance that is too high to meet other specification requirements.

The e.m.f. equation is often combined with the expression for inductance, L, to give a relation that is independent of the number of turns.

$$N^2 = \frac{2E^2}{\omega^2 \hat{B}_e^2 A_e^2} = \frac{L l_e}{\mu_o \mu_e A_e}.$$

Therefore,

$$A_e l_e = V_e = \frac{2\mu_o \mu_e E^2}{\omega^2 L \hat{B}_e^2} \quad m^3. \qquad \ldots(12)$$

where l_e is the effective magnetic length of the core, and V_e is the effective volume of the core.

This equation gives the core volume required to satisfy simultaneously the flux density and inductance requirements. However, an inspection of this relation shows that caution is required in its use. It states that the higher the effective permeability or the lower the required inductance the larger is the required core volume. This surprising result is obtained because the inductance has been given a specific value rather than a minimum value. Thus if for a given frequency, voltage and flux density the inductance is fixed at a very low value the required core volume may be very large. The cross-sectional area of the core must be large enough to satisfy the flux density requirements but at the same time the core reluctance must be high so that the shunt inductance is not exceeded; for a given value of μ_e this may mean that the magnetic path length must be long to obtain the required high reluctance, hence the large volume. Alternatively the core volume may be kept within reasonable limits by reducing μ_e, by introducing an air gap, for example. This would be the right course in the design of a tuned transformer requiring a specified shunt inductance value. However, for a normal power or wideband transformer it offers no advantage; an excessive shunt inductance in these cases is detrimental only inasmuch as it may cause the leakage inductance or winding resistance to be too high, and these parameters are unaffected by a reduction of μ_e.

Eq. 12 is often quoted. The above discussion has shown that it can lead to unexpected results. If the flux density and inductance are the main consideration in a design then it is probably better to consider them separately. If the flux density is the limiting parameter, due to core loss or saturation, then for a given core the minimum number of turns is determined by Eq. 11. The shunt inductance may then be calculated from

$$L = \frac{\mu_o \mu_e N^2 A_e}{l_e} \quad H.$$

Since it was postulated that the design was flux density limited, the inductance will be greater than the minimum required to meet the magnetizing current or transmission band specification. The leakage inductance and resistance may then be estimated (Ref. 8); if they are excessive it may be necessary to use a larger core. If, on the other hand, the design is inductance limited the required shunt inductance will determine the number of turns, and the resultant flux density will be acceptable. At the start of a design it may not be known which is the limiting parameter so the number of turns is calculated by both criteria and the larger number is used.

In connection with these basic calculations it should be noted that the core permeability is a function of flux density and in power transformers the amplitude permeability at the maximum working flux density may be appreciably larger than the initial permeability. Which value of permeability is used depends on whether the transformer is to be operated only at the rated voltage or whether it must give a satisfactory performance at voltages down to zero. If the latter requirement applies the initial permeability must be used.

Continuing the discussion of general design considerations some basic relations concerning power will now be considered.

It is often stated that for maximum efficiency in a transformer the core loss should equal the winding losses. This arises from the following argument based on the equivalent circuit shown in Fig. 5. Assuming that

$$R_1 + R'_2 \ll R'_b \ll |L_p \text{ and } R_p \text{ in parallel}|,$$

the winding and core losses are given by:

$$\left.\begin{aligned} \text{winding loss} &= P_w = I_1^2(R_1 + R'_2) \quad W \\ \text{core loss} &= P_m V_e = U_1^2/R_p \quad W \end{aligned}\right\} \ldots(13)$$

where P_m is the core loss density and

V_e is the effective core volume

and the power in the load is

$$P_b = I_1^2 R'_b = U_1^2/R'_b.$$

Therefore

$$\frac{P_w + P_m V_e}{P_b} = \frac{R_1 + R'_2}{R'_b} + \frac{R'_b}{R_p}. \qquad \ldots(14)$$

This expression for the ratio of the total power loss to the output power may be differentiated with respect to R'_b to obtain the condition for minimum power loss. This condition is that $(R_1 + R'_2)/R'_b = R'_b/R_p$, that is, the value of load resistance is such that the core loss equals the winding loss. This result is not valid generally because if the output power is constant the applied voltage will depend on R'_b and so, consequently, will the flux density. Under these conditions R_p, the core loss resistance, will not, in general, be constant.

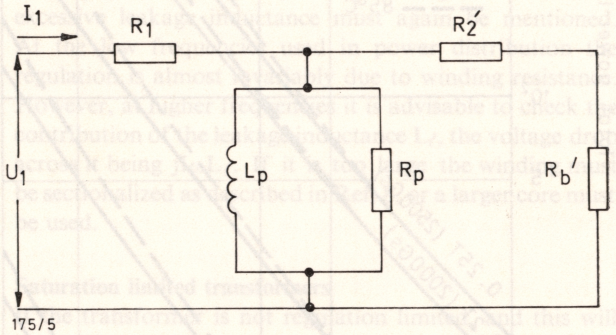

Fig. 5—Simplified equivalent circuit of a power transformer the elements referred to the primary side

U_1 = Primary voltage
R_1 = Primary winding resistance
I_1 = Primary current
R'_2 = Secondary winding resistance
R'_b = Load resistance
L_p = Shunt inductance of primary
R_p = Shunt core loss resistance

The more practical situation is the design of a transformer on a given core to give minimum total power loss when delivering a given power into a given load. The number of primary turns, N_1, is the variable. It may be shown that if $P_m V_e \propto \hat{B}_e^n$ then the minimum power loss occurs when

$$P_m = \frac{2}{n} P_w. \qquad \ldots(15)$$

It has been mentioned that the value of n lies between about 2 and 3; only when it is 2 does the equating of the core and winding losses give minimum total loss.

It is not always possible or desirable to apply this result. As described at the beginning of this section, low frequency power transformer designs are often regulation or saturation limited; under these conditions the winding loss predominates. At higher frequencies where the design is limited by core loss (temperature rise) it is possible to choose the most suitable ratio of core and winding loss. When small size is more important than efficiency it is usual for transformers with laminated iron cores to be designed to have high core loss relative to the winding loss. The resulting heat may be removed from the core by conduction to a heat sink, so the core temperature is prevented from being excessive.

The calculation of winding resistance and the optimum ratio of primary and secondary winding areas are discussed

---

(Eq. 11) $E = \frac{\omega \hat{B}_e A_e N 10^{-8}}{\sqrt{2}}$ V.

*The effective core parameters are normally quoted in the data sheets. They are also defined in Ref 7.

(Eq. 12) $A_e l_e = V_e = \frac{8\pi \mu_e E^2 10^7}{\omega^2 L \hat{B}_e^2}$ cm³.

in Ref. 7. Data on the losses in ferrite cores at high flux densities are given in Fig. 6.

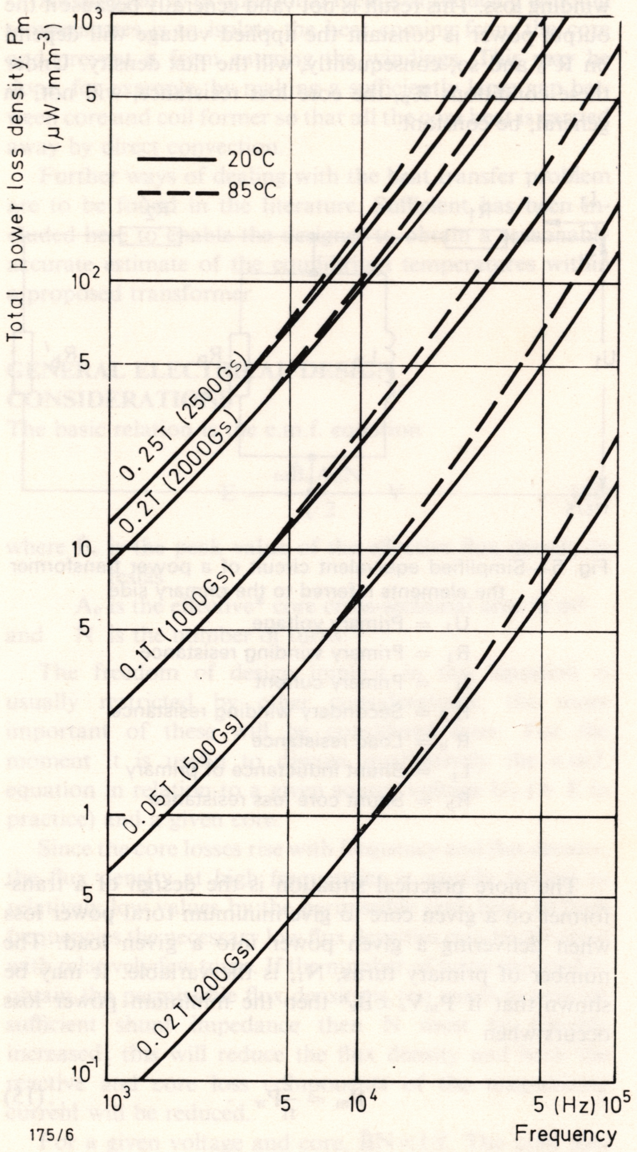

Fig. 6—Total power loss density as a function of frequency at high flux densities for transformer cores FX3234 and FX3235

LOW FREQUENCY POWER TRANSFORMERS

General

The transformers to be considered under this heading are those for which the winding resistance may be taken as substantially equal to the d.c. value. The frequency at which this ceases to be true depends on the output power; for example, a 1kW transformer may have an appreciable increase of winding resistance due to eddy currents at frequencies above about 3kHz. The problems peculiar to the design of these higher frequency transformers are considered in later sections.

It was shown in the previous section that the design of a power transformer is dominated by the permissible flux density. At very low frequencies it is usually the saturation flux density that limits the design while at higher frequencies it is usually the flux density corresponding to the permissible core loss. Given a limit value for the flux density, the design of a transformer on a given core may be very straightforward. The number of primary turns may be calculated from Eq. 11 in which E is put equal to the primary voltage. The number of turns on the other windings may be provisionally calculated from the specified voltage ratios. The conductor diameters and resistances may readily be calculated by the usual methods (for example, Ref. 7). The internal voltage drops due to winding resistances and, if significant, the leakage inductance may then be calculated, and the number of secondary turns may be increased if necessary to obtain the specified full load secondary voltages.

At this stage of the design it may be found that the winding resistance is too high, leading either to excessive regulation or to excessive power loss in the windings. If so, a larger core must be selected and the design repeated.

When the design satisfies the flux density and winding loss requirements, the shunt inductance should be calculated to ensure that it is adequate to meet the specification for magnetizing current or possibly return loss.

This trial and error approach can, with experience, lead quite quickly to a satisfactory design. However it is helpful to have some advance information of the powerhandling capacity of available cores. In the following sections the three main classes of design are analysed with the object of providing core parameters that will enable the most suitable core to be rapidly selected.

Regulation limited transformers

Because regulation becomes a limitation only at very low frequencies it is rarely a factor in the design of ferrite-cored transformers. However, the following analysis may be useful in certain circumstances.

The voltage regulation may be defined as the difference between the output voltage on open circuit and that on full load, expressed as a fraction or percentage of the open circuit voltage. From Fig. 5 the voltage regulation due to the winding resistance, referred to the primary side, is given by

$$\text{Voltage regulation} \approx \frac{I_1(R_1+R'_2)}{U_1} = \frac{I_1^2(R_1+R'_2)}{\text{input power}}$$

If the winding loss, $I_1^2(R_1+R'_2)$, is denoted by P_w and P_i and P_o denote the input and output power respectively, then for a voltage regulation of x per cent:

$$\frac{x}{100} = \frac{P_w}{P_i}\ .$$

Therefore

$$P_i = P_w.\frac{100}{x}\ .$$

Therefore

$$P_o = P_i - P_w = P_w\left(\frac{100}{x} - 1\right)\ \text{W} \quad . \quad \ldots(16)$$

Assuming that the transformer has two windings and that each has the same cross-sectional area then it is easily shown that

$$R_1 = \frac{2m\rho_c N_1^2 l_w}{A_a F_a}\ \Omega$$

where ρ_e is the conductor resistivity at 20°C,

A_a is the total window area,
F_a is the corresponding copper factor and
m is the fractional increase of conductor resistivity above the value at 20°C. For values of m see caption of Table 3.

Therefore,

$$R_1 + R_2' = \frac{4m\rho_c N_1^2 l_w}{A_a F_a}\ \Omega \quad . \quad \ldots(17)$$

Therefore,

$$P_w = \frac{4I_1^2 m\rho_c N_1^2 l_w}{A_a F_a}\ \text{W} \quad . \quad \ldots(18)$$

The number of turns may be eliminated by substitution from Eq. 11 putting $U_1 = E$. Thus

$$P_w = \frac{8I_1^2 U_1^2 m\rho_c l_w}{A_e^2 A_a F_a \omega^2 \hat{B}_e^2}\ \text{W}$$

$$\left.\begin{aligned} &= \frac{P_i^2 m k_1}{f^2 \hat{B}_e^2}\ \text{W} \\ \text{where}\quad k_1 &= \frac{2\rho_c l_w}{\pi^2 A_e^2 A_a F_a}\ \Omega.\text{m}^{-4}. \end{aligned}\right\} \quad \ldots(19)$$

But

$$P_w = P_i.\frac{x}{100}\ .$$

Therefore,

$$P_i = \frac{f^2 \hat{B}_e^2}{m k_1}.\frac{x}{100}\ .$$

It is easily shown from the definition of x or by Eq. 16 that

$$P_i = \frac{P_o}{1 - \dfrac{x}{100}}\ .$$

Therefore,

$$P_o = \frac{f^2 \hat{B}_e^2}{m k_1}.\frac{(x - 0{\cdot}01x^2)}{100}\ \text{W} \quad \ldots(20)$$

or

$$k_1 = \frac{f^2 \hat{B}_e^2}{m P_o}.\frac{(x - 0{\cdot}01x^2)}{100}\ \Omega.\text{m}^{-4}. \quad \ldots(21)$$

If the regulation is 10%

$$k_1 = 0{\cdot}09\frac{f^2 \hat{B}_e^2}{m P_o}\ .$$

For a given core material, $\hat{B}_e^2$ is limited to a value determined by the saturation flux density; the frequency, the required output power and the permissible regulation are given parameters in the design. Therefore the design value of k_1 may be obtained from Eq. 21. It is then necessary to find a core having a value of k_1 (from Eq. 19) that is equal to or smaller than the design value. The core selection is facilitated if the available cores are tabulated with their k_1 values. Table 3, which is introduced later, gives data for a range of ferrite cores suitable for power transformers. It includes values of k_1 calculated on the assumption that the overall copper factor, F_a, is 0·30.

Finally the possibility of poor regulation due to excessive leakage inductance must again be mentioned. At the low frequencies used in power distribution the regulation is almost invariably due to winding resistance. However, at higher frequencies it is advisable to check the contribution of the leakage inductance L_ℓ, the voltage drop across it being $jI\omega L_\ell$. If it is too large the winding must be sectionalized as described in Ref. 8, or a larger core must be used.

Saturation limited transformers

If the transformer is not regulation limited, and this will be true for most ferrite-cored power transformers, then the next limitation encountered is that imposed by the saturation of the core. The core is operated at a flux density, $\hat{B}_e$, which is suitably less than the saturation value, and the core loss, P_m, is less than the value dictated by temperature rise.

The following method of core selection has been proposed (Ref. 9). To any given core plus winding, a nominal value of the total power dissipation, P_{tot}, may be assigned. This assumes a certain standard of cooling, such as free air convection and radiation from all exposed surfaces of the core and winding, and it assumes a certain permissible temperature rise. In the present treatment, P_{tot} is taken as corresponding to a uniform rate of heat transfer of 300μW.mm^{-2} (approx. 0·2 W.in^{-2}) from all the exposed surfaces. Expressed in terms of the core and winding losses,

$$P_{tot} = P_m V_e + P_w$$

$$= P_m V_e + \frac{P_i^2 m k_1}{f^2 \hat{B}_e^2}\ ,$$

from Eq. 19.

Therefore, $$P_{tot} \approx P_m V_e + \frac{P_o^2 m k_1}{f^2 \hat{B}_e^2}\ \text{W} \quad \ldots(22)$$

since, for a reasonably efficient transformer,

$$P_i \approx P_o.$$

For a given core made of a specified material, the core loss, P_m, is determined when f and $\hat{B}_e$ are determined. Thus corresponding to the value of P_{tot} there is a value of P_o which is the output rating of the core at a specified frequency. It depends on the geometry and material of the core and winding but is substantially independent of the number of turns. This nominal output power may be calculated for a suitable range of cores and the tabulated results would be a useful guide to the selection of a core for a saturation limited transformer. In practice allowance would have to be made if (1) the rate of cooling or the permissible temperature rise were different from the values assumed, and (2) if the copper factor were other than the average value used in calculating k_1. (For example, a high

---

(Eq. 19) $P_w = \dfrac{P_i^2 m k_1}{f^2 B_e^2}$ W

where $k_1 = \dfrac{2\rho_c l_w 10^{16}}{\pi^2 A_e^2 A_a F_a}$ Ω.cm^{-4}.

voltage transformer or a transformer having many windings would have a copper factor that was smaller than average.)

Since both terms of Eq. 22 depend on frequency, a tabulation of P_o is only practical for cores that are used at a standard frequency, for example, silicon iron laminated cores for 50 or 60Hz, or strip wound cut cores (C cores) for 400Hz. As ferrite cores may be used over a wide frequency range, P_o cannot be given as a core parameter for ferrite cores. However if P_m can be expressed as a function of frequency then a graph of P_o against frequency may be constructed for a given core. If, for example, the energy lost in a unit volume of the core is w_m joules per cycle, then

$$P_{tot} = w_m V_e f + P_o^2 \frac{mk_1}{f^2 \hat{B}_e^2} \;.$$

Therefore

$$P_o^2 = (P_{tot} - w_m V_e f)\frac{f^2 \hat{B}_e^2}{mk_1} \quad W \;. \qquad \ldots(23)$$

This method of expressing core performance is illustrated in the introduction to Table 3 where a representative range of cores is considered.

Core loss limited transformers

At frequencies above about 1kHz the design of a ferrite-cored power transformer ceases to be governed by the saturation flux density; the core loss limits the flux density to a value lower than that corresponding to the onset of saturation.

It was shown that for maximum efficiency the core loss should equal (2/n) × the winding loss, where n is the Steinmetz exponent (see Eq. 15) and lies between approximately 2 and 3. It was also observed that practical considerations may lead to a loss ratio other than this optimum. For the purpose of calculating design parameters it is reasonable to assume that the core and winding losses will be equal. The results will not be appreciably affected by a moderate departure from equality; the exact loss ratio will emerge during the final design calculations.

Given a suitable core the design procedure is, as before, quite straightforward. The total permissible loss is decided on heating considerations. If half is allocated to the core, the permissible core loss density is determined. Since this depends on f and $\hat{B}_e$ the latter is readily obtained from graphs such as those in Fig. 6. The core parameters and the e.m.f. Eq. 11 will enable the number of turns to be calculated. From this the conductor diameter and copper loss may be obtained. The main difficulty again is that at the start of a design it is not known which core size is the most suitable.

The following procedure is based on a method suggested by MacFadyan (Ref. 9) and it enables the designer to select from a range of cores one which will have approximately the required performance. It is necessary to know only the output power, P_o, and to estimate the overall copper factor and a core loss parameter.

From Eq. 18 the total winding loss referred to the primary side is

$$P_w = \frac{4I_1^2 m\rho_c N_1^2 l_w}{A_a F_a} \quad W \;.$$

For equal core and winding loss,

$$P_w = P_m V_e = \frac{P_{tot}}{2}.$$

Therefore,

$$\frac{4I_1^2 m\rho_c N_1^2 l_w}{A_a F_a} = \frac{P_{tot}}{2}.$$

The output power is very nearly equal to $I_1^2 R_b'$, therefore by substituting P_o/R_b' for I_1^2, the following expression is obtained:

$$P_o = \frac{P_{tot}}{8} \cdot \frac{R_b' A_a F_a}{m\rho_c N_1^2 l_w} \quad W \;. \qquad \ldots(24)$$

The number of turns must be eliminated. This may be done by introducing the core loss in terms of some convenient parameter. Such a parameter is a normalized value of the shunt core loss resistance, R_p, and this may be obtained as follows.

The total core loss $= P_m V_e = U_1^2/R_p$. Using the e.m.f. Eq. 11 to eliminate U_1^2, (assuming that $U_1 = E$):

$P_m V_e R_p = 2\pi^2 \hat{B}_e^2 A_e^2 N_1^2 f^2$ for sinusoidal voltages.

For a given frequency, flux density and core loss density

$$R_p = \frac{2\pi^2 \hat{B}_e^2 f^2}{P_m} . N_1^2 A_e \quad \Omega \qquad \ldots(25)$$

since $V_e = A_e . l_e$.

This shunt resistance may be normalized to a value corresponding to one turn on a core having C_1 ($= l_e/A_e$) equal to $1m^{-1}$. If this value is denoted by $(R_p)_1$ then

$$\left.\begin{aligned} (R_p)_1 &= \frac{2\pi^2 \hat{B}_e^2 f^2}{P_m} \quad \Omega . m^{-1} \\ \text{and} \qquad & \\ R_p &= (R_p)_1 \frac{N_1^2}{C_1} \quad \Omega \end{aligned}\right\} \qquad \ldots(26)$$

It has been seen that the power loss in a core is approximately proportional to B_e^n.
Therefore

$$\frac{U_1^2}{R_p} \propto B_e^n \propto U_1^n \text{ at a given frequency.}$$

For ferrites suitable for power transformer applications it is found that usually $n \approx 2$. Therefore for these materials R_p and $(R_p)_1$ are approximately independent of flux density up to values approaching saturation. If there is eddy current loss in the core this is proportional to $\hat{B}_e^2$ and thus enhances the constancy of R_p.

(Eq. 25) $\quad R_p = \frac{2\pi^2 \hat{B}_e^2 f^2}{P_m} . \frac{N_1^2 A_e}{l_e} . 10^{-16} \quad \Omega$

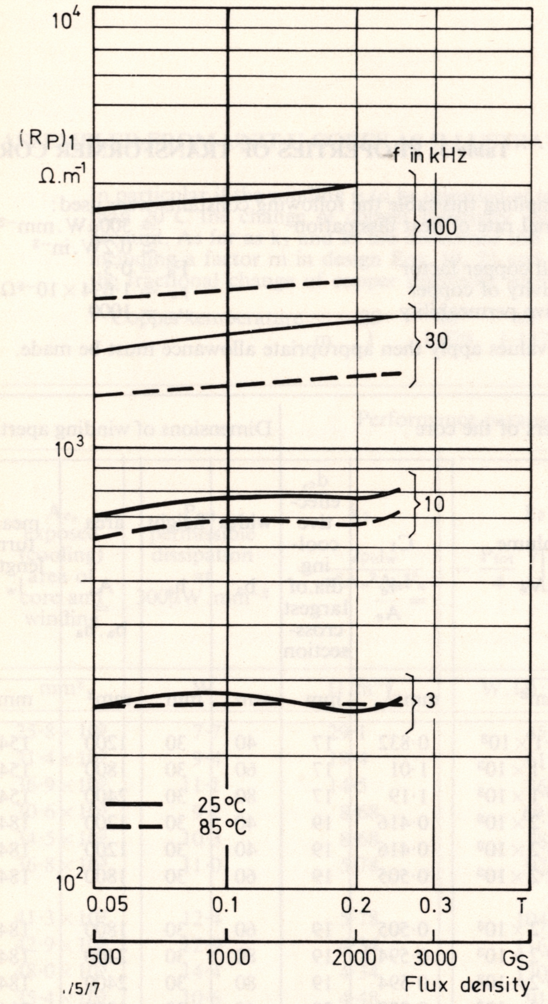

Fig. 7—Normalized shunt core loss resistance $(R_p)_1$, (that is, R_p when $N = 1$ and $C_1 = 1m^{-1}$) as a function of flux density at various frequencies for a transformer grade of manganese zinc ferrite

Fig. 7 shows $(R_p)_1$ as a function of flux density calculated at various frequencies from the data given in Fig. 6, appropriate allowance having been made for the eddy current loss in a core having an assumed 15 × 15mm cross section. The higher the value of $(R_p)_1$ the more suitable is the material. To the extent that the curves are approximately horizontal it is relatively easy to estimate $(R_p)_1$ at a given frequency with reasonable accuracy in spite of the fact that the flux density to be used is unknown.

It is now possible to eliminate N_1 from Eq. 24. From Eq. 26

$$P_m V_e = \frac{U_1^2}{R_p} = \frac{U_1^2 l_e}{(R_p)_1 N_1^2 A_e}$$

$$= \frac{P_{tot}}{2} \text{ for equal core and winding losses.}$$

Therefore

$$N_1^2 = \frac{2U_1^2 l_e}{P_{tot}(R_p)_1 A_e} \;.$$

This may be substituted in Eq. 24 so that

$$P_o = \frac{P_{tot}^2 R_b'}{16U_1^2} \cdot \frac{F_a (R_p)_1 A_e A_a}{m\rho_c l_e l_w} \;.$$

Since $U_1^2/R_b' = P_o$:

$$P_o \sqrt{\left[\frac{m}{F_a (R_p)_1}\right]} = \frac{P_{tot}}{4}\sqrt{\left[\frac{A_e A_a}{\rho_c l_e l_w}\right]} = k_2 \quad W . \Omega^{-\frac{1}{2}} . m^{\frac{1}{2}} \qquad \ldots(27)$$

The constant k_2 is a property of the core geometry, and values may be listed for suitable cores. It is then only necessary to calculate $P_o[m/F_a(R_p)_1]^{\frac{1}{2}}$; the output power is specified in the design requirements, the overall copper factor may be estimated by the designer (it is usually between 0·25 and 0·35), m depends on the working temperature (see caption of Table 3) and $(R_p)_1$ may be estimated from a graph such as that in Fig. 7. A core may then be selected such that it has k_2 equal to or larger than this calculated value. In the next section this and the foregoing procedures are applied to a range of cores and their performance is discussed.

Core performance

In the preceding sections parameters have been derived which, if they were made available for various ferrite cores, would facilitate the selection of the core most suitable to meet a given requirement. A difficulty is that, whereas there are standard ranges of silicon iron cores, there has, hitherto, been no recognised range of ferrite cores designed specifically for power transformers. However, as a result of the work reported here, such a range of cores was devised and is now commercially available. It is based on various assemblies of square-section ferrite U-cores. There are two unit U-cores, FX3234 and FX3235, the only difference being that one has longer legs than the other. They are illustrated in Fig. 8 together with two typical assemblies. The unit U cores have been dimensioned and proportioned in such a way that the assemblies are not too far from the shape that is optimum for least R_{dc}/L and total loss. Although this range is, to some extent, arbitrary it may be regarded as realistic and it does cover a useful range of sizes.

Data for this range of cores are given in Table 3. In addition to the usual dimensional parameters of the core and winding space, a number of performance parameters are given. The first of these is the exposed surface area, A_c, of the core plus a full winding, that is, the total available cooling area. From this the value of the nominal power dissipation, P_{tot}, has been calculated assuming a uniform heat transfer of 300μW.mm⁻² (approx. 0·2W.in⁻²). The next column lists the values of k_1 (see Eq. 19) using $\rho_c = 1{\cdot}694 \times 10^{-8}\Omega.m$ and $F_a = 0{\cdot}3$. Values of k_2 from Eq. 27 are then given. The next two columns give parameters relevant to the resistance/inductance ratio. The first is $k_3 = 2\rho_c l_e l_w/\mu_o A_e A_a$ where l_w is the mean turn length of the windings. This parameter equals $(R_{dc}/L)_{\frac{1}{2}}$ normalized with respect to μ_e and F_a; that is, it depends only

Table 3. PROPERTIES OF TRANSFORMER CORES ASSEMBLED FROM UNIT U CORES AS ILLUSTRATED IN FIG. 8

In compiling this table the following constants were used:

Nominal rate of heat dissipation $= 300\mu W.mm^{-2}$
$\approx 0{\cdot}2W.in^{-2}$
Overall copper factor $F_a = 0{\cdot}3$
Resistivity of copper $\rho_c = 1{\cdot}694 \times 10^{-8}\Omega.m$
Effective permeability $\mu_e = 1000$

If other values apply then appropriate allowance must be made.

In particular if the winding is to be operated at temperatures other than 20°C the change of copper resistivity should be taken into account. As far as k_1 and k_3 are concerned this has been done by including a factor m in design Eqs. 19, 23 and 27. This factor is the fractional change of copper resistivity with temperature:

Copper temperature	20	40	60	80	100°C
m	1	1·079	1·157	1·236	1·314

	Physical dimensions (see Fig. 8)					Dimensional parameters of the core					Dimensions of winding aperture			
Core ref.	A	B	C	D	E	Magnetic: length l_e	area A_e	volume V_e	$C_1 = \frac{l_e}{A_e}$	d_c, effective cooling dia. of largest cross-section	width b_a	height h_a	area $A_a = b_a . h_a$	mean turn length l_w
	mm					mm	mm²	mm³	mm⁻¹	mm	mm	mm	mm²	mm
SSU1	60	70	15	75	90	187	225	$42{\cdot}1\times10^3$	0·832	17	40	30	1200	154
SLU1	60	90	15	75	90	227	225	$51{\cdot}1\times10^3$	1·01	17	60	30	1800	154
LLU1	60	110	15	75	90	267	225	$60{\cdot}1\times10^3$	1·19	17	80	30	2400	154
SSU2	60	70	30	90	90	187	450	$84{\cdot}2\times10^3$	0·416	19	40	30	1200	184
SSE1	120	70	15	75	—	187	450	$84{\cdot}2\times10^3$	0·416	19	40	30	1200	184
SLU2	60	90	30	60	90	227	450	$102{\cdot}2\times10^3$	0·505	19	60	30	1800	184
SLE1	120	90	15	75	—	227	450	$102{\cdot}2\times10^3$	0·505	19	60	30	1800	184
LLU2	60	110	30	90	90	267	450	$120{\cdot}2\times10^3$	0·594	19	80	30	2400	184
LLE1	120	110	15	75	—	267	450	$120{\cdot}2\times10^3$	0·594	19	80	30	2400	184
SSU3	60	70	45	105	90	187	675	$126{\cdot}3\times10^3$	0·277	20	40	30	1200	214
SLU3	60	90	45	105	90	227	675	$153{\cdot}3\times10^3$	0·337	20	60	30	1800	214
SSU4	60	70	60	120	90	187	900	$168{\cdot}4\times10^3$	0·208	20·5	40	30	1200	244
SSE2	120	70	30	90	—	187	900	$168{\cdot}4\times10^3$	0·208	34	40	30	1200	214
LLU3	60	110	45	105	90	267	675	$180{\cdot}3\times10^3$	0·396	20	80	30	2400	214
SLU4	60	90	60	120	90	227	900	$204{\cdot}4\times10^3$	0·252	20·5	60	30	1800	244
SLE2	120	90	30	90	—	227	900	$204{\cdot}4\times10^3$	0·252	34	60	30	1800	214
LLU4	60	110	60	120	90	267	900	$240{\cdot}4\times10^3$	0·297	20·5	80	30	2400	244
LLE2	120	110	30	90	—	267	900	$240{\cdot}4\times10^3$	0·297	34	80	30	2400	214
SSE3	120	70	45	105	—	187	1350	$252{\cdot}6\times10^3$	0·139	36	40	30	1200	244
SLE3	120	90	45	105	—	227	1350	$306{\cdot}6\times10^3$	0·168	36	60	30	1800	244
SSE4	120	70	60	120	—	187	1800	$336{\cdot}8\times10^3$	0·104	38	40	30	1200	274
LLE3	120	110	45	105	—	267	1350	$360{\cdot}6\times10^3$	0·198	36	80	30	2400	244
SLE4	120	90	60	120	—	227	1800	$408{\cdot}6\times10^3$	0·126	38	60	30	1800	274
LLE4	120	110	60	120	—	267	1800	$480{\cdot}6\times10^3$	0·148	38	80	30	2400	274

Performance parameters									
A_c, exposed (cooling) area of core and winding	P_{tot}, permissible dissipation at $300\mu W.mm^{-2}$	$k_1 = \frac{2\rho_c l_w}{\pi^2 A_e^2 A_a F_a}$	$k_2 = \frac{P_{tot}}{4}\sqrt{\left[\frac{A_e A_a}{\rho_c l_e l_w}\right]}$	$k_3 = \frac{2\rho_c l_e l_w}{\mu_0 A_e A_a}$	$\left[\frac{R_{dc}}{L}\right]^{\frac{1}{2}} = \frac{k_3}{\mu_e F_a}$	ψ, figure of merit	Approx. weight of core	Approx. weight of core and winding	Core ref.
mm²	W	$\Omega.m^{-4}$	$W.\Omega^{\frac{1}{2}}.m^{\frac{1}{2}}$	$\Omega.H^{-1}$	$\Omega.H^{-1}$	—	kg	kg	
$25{\cdot}8\times10^3$	7·7	29·1	45·3	2882	9·61	495	0·22	0·72	SSU1
$31{\cdot}4\times10^3$	9·4	19·4	61·4	2332	7·77	474	0·26	1·0	SLU1
$36{\cdot}9\times10^3$	11·1	14·5	76·8	2058	6·86	477	0·30	1·3	LLU1
$30{\cdot}6\times10^3$	9·2	8·68	69·8	1722	5·74	334	0·43	1·0	SSU2
$34{\cdot}5\times10^3$	10·3	8·68	78·3	1722	5·74	469	0·43	1·0	SSE1
$36{\cdot}8\times10^3$	11·0	5·78	92·9	1392	4·64	319	0·52	1·4	SLU2
$41{\cdot}3\times10^3$	12·4	5·78	104	1392	4·64	449	0·52	1·4	SLE1
$42{\cdot}9\times10^3$	12·9	4·34	116	1228	4·10	322	0·60	1·8	LLU2
$48{\cdot}0\times10^3$	14·4	4·34	130	1228	4·10	453	0·60	1·8	LLE1
$35{\cdot}4\times10^3$	10·6	4·48	91·3	1334	4·45	287	0·65	1·3	SSU3
$42{\cdot}2\times10^3$	12·6	2·99	121	1080	3·60	274	0·78	1·8	SLU3
$40{\cdot}2\times10^3$	12·1	2·88	112	1140	3·80	268	0·86	1·7	SSU4
$40{\cdot}2\times10^3$	12·1	2·52	120	1000	3·33	308	0·86	1·6	SSE2
$48{\cdot}9\times10^3$	14·7	2·24	150	952	3·17	277	0·91	2·3	LLU3
$47{\cdot}6\times10^3$	14·3	1·92	148	924	3·08	256	1·0	2·2	SLU4
$47{\cdot}6\times10^3$	14·3	1·68	158	910	2·70	295	1·0	2·1	SLE2
$54{\cdot}9\times10^3$	16·5	1·44	182	914	2·71	259	1·2	2·8	LLU4
$54{\cdot}9\times10^3$	16·5	1·26	194	714	2·38	297	1·2	2·6	LLE2
$45{\cdot}9\times10^3$	13·8	1·28	157	760	2·54	259	1·3	2·1	SSE3
$53{\cdot}9\times10^3$	16·2	0·852	205	616	2·05	248	1·6	2·7	SLE3
$51{\cdot}6\times10^3$	15·5	0·807	193	640	2·14	239	1·7	2·6	SSE4
$61{\cdot}8\times10^3$	18·6	0·639	251	542	1·81	250	1·8	3·4	LLE3
$60{\cdot}2\times10^3$	18·0	0·538	250	518	1·73	229	2·1	3·4	SLE4
$68{\cdot}7\times10^3$	20·6	0·404	304	458	1·52	230	2·4	4·2	LLE4

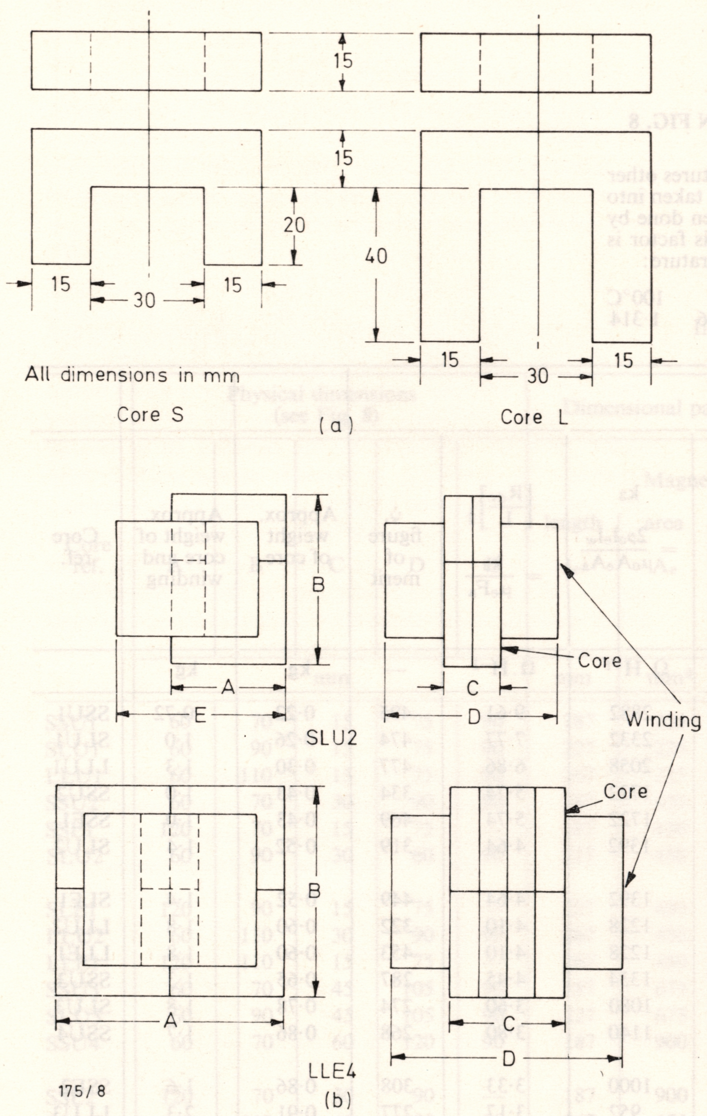

Fig. 8—Unit U-cores. (a) Dimensions of the two unit cores, in mm. (b) Definition of overall dimension symbols used in Table 3, and illustration of assembly code

Assembly code:

S—short U-core

L—long U-core

First two letters indicate which of the three possible combinations of S and L is used

The third letter is U for the single aperture core and E for the double aperture core

The final cypher is the number of U-cores stacked side by side in the assembly

on the geometry of the core. The second is $(R_{dc}/L)_{\frac{1}{2}}$, that is, the d.c. resistance/inductance ratio for a winding that occupies half the winding space, assuming that the overall copper factor, F_a, of the half winding space is 0·3 and $\mu_e = 1000$. The next column lists a figure of merit, ψ. This is proportional to R_{dc}/L when this ratio is made independent of the volume of the smallest rectangular box that will enclose the core plus winding; a low ψ indicates a good core shape. Finally approximate weights of core and core plus winding are given.

For regulation limited transformers k_1 is the relevant parameter. From Eq. 21, k_1 is calculated using the specified frequency, flux density, output power and regulation, and a core is selected which has a value of k_1 equal to or less than the calculated value. The flux density is determined by the saturation and is often taken as that flux density at which the amplitude permeability has fallen to a value equal to the initial permeability at a typical working temperature. Fig. 9 shows the B-H loops and the $\mu_a - \hat{B}$ curves for the ferrite U cores FX3234 and FX3235. A suitable working value of saturation flux density is about 0·3T (3000Gs).

The parameter k_1 is also used in saturation limited transformers, see Eq. 23. Again $\hat{B}_e$ is determined by the core saturation and may be taken as 0·3T (3000Gs) at a typical working temperature. To calculate P_o, the value of w_m must be estimated. At low frequencies the value of w_m at $\hat{B}_e = 0{\cdot}3$T (3000Gs) and a temperature of 85°C is typically 18.10^{-9} J.mm^{-3}.cycle^{-1}. Using these figures P_o has been calculated as a function of frequency for each of the listed transformer cores and the results are shown in Fig. 10. These curves provide a means of selecting a core to transmit a given power at a given frequency. Over the range of frequencies occupied by these curves the winding loss predominates and the core loss is limited by the saturation of the core. Each curve is terminated at the upper end at the frequency at which the core loss has risen to equal the winding loss. Beyond this frequency the design is core loss limited.

If the heat transfer from the transformer differs from the value used in calculating P_{tot}, that is, 300μW.mm^{-2} (0·2W.in^{-2}) allowance must be made for this. It is not easy to make an allowance in such a way that the curves of Fig. 10 can still be used. However, when the core loss is negligible Eq. 23 shows that $P_o{}^2 \propto P_{tot} f^2$, that is, the curves of Fig. 10 have unity slope; the falling off at the upper end is due to the increasing core loss. If the heat dissipation is a factor k greater than the assumed value then P_{tot} is increased by the same factor and, where the core loss is negligible, P_o is increased by the factor $\sqrt{k}$. Therefore Fig. 10 may still be useful in estimating the core size provided (1) the specified value of P_o is divided by $\sqrt{k}$ before being used to select a core and (2) the droop due to core loss is disregarded, that is, the curves are extrapolated with unity slope. With the increased dissipation the core loss will remain negligible up to higher frequencies and therefore the droops and the terminating points (at which the core loss has risen to $P_{tot}/2$) will be removed to higher frequencies.

As observed earlier, silicon iron cores are used for power frequency transformers due to their higher values of saturation flux density, thus over much of the lower frequency range of Fig. 10 the curves for the ferrite cores would indicate a lower output power than corresponding curves for silicon iron. To give an indication of the extent of this region, the nominal output power, P_o, has been recalculated for each of the cores in Table 3 on the assumption that the core material was 0·004in (0·1mm) grain oriented silicon steel having a loss that is typical of strip-

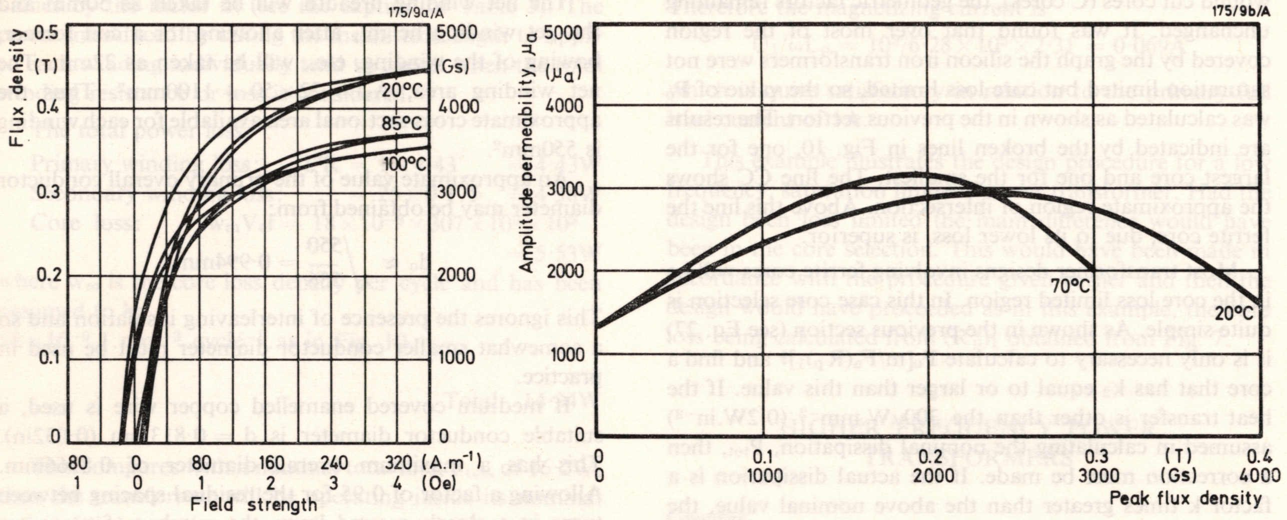

Fig. 9—B-H loops and μ_a-$\hat{B}$ curves for the ferrite U-cores FX3234 and FX3235

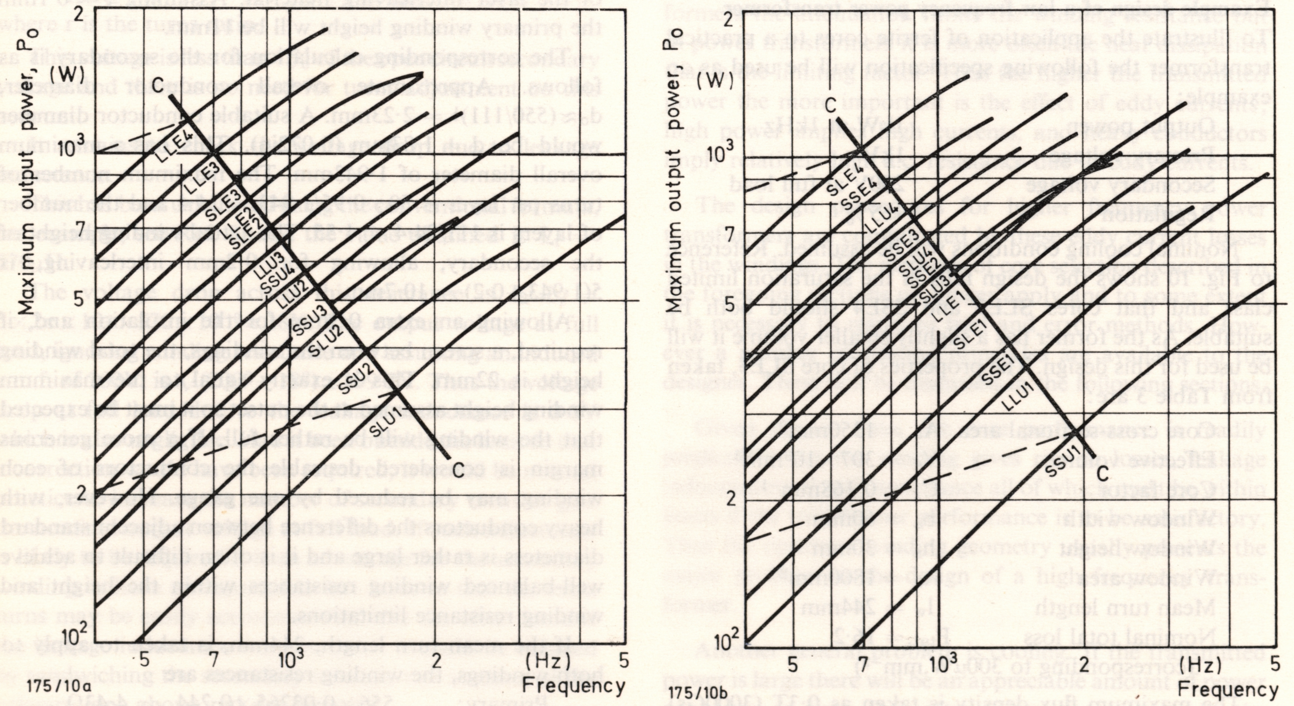

Fig. 10—The performance of saturation limited ferrite transformers

The nominal value of P_o, the maximum output power, as a function of frequency for the 24 core assemblies listed in Table 3. The computation uses Eq. 23 and assumes $w_m = 18.10^{-9}$ J.mm^{-3}.cycle^{-1} at $B_e = 0{\cdot}3$T, that the nominal cooling rate of 300μW.mm^{-3} applies, that the overall copper factor F_a is 0·3 and that the core temperature is 20°C. The curves are terminated at the upper end at the frequency at which the core loss equals the winding loss; at higher frequencies the design would be loss limited. The line CC indicates the approximate region below which 0·004 in grain oriented silicon steel cores of equivalent size have superior performance. The broken lines indicate the course of the P_o curves for such cores wound cut cores (C cores), the geometric factors remaining unchanged. It was found that over most of the region covered by the graph the silicon iron transformers were not saturation limited but core loss limited, so the value of P_o was calculated as shown in the previous section. The results are indicated by the broken lines in Fig. 10, one for the largest core and one for the smallest. The line CC shows the approximate region of intersection. Above this line the ferrite core, due to its lower loss, is superior.

Most transformer designs involving ferrite cores will be in the core loss limited region. In this case core selection is quite simple. As shown in the previous section (see Eq. 27) it is only necessary to calculate $P_o[m/F_a(R_p)_1]^{\frac{1}{2}}$ and find a core that has k_2 equal to or larger than this value. If the heat transfer is other than the 300μW.mm^{-2} (0·2W.in^{-2}) assumed in calculating the nominal dissipation, P_{tot}, then a correction must be made. If the actual dissipation is a factor k times greater than the above nominal value, the figure obtained from $P_o[m/F_a(R_p)_1]^{\frac{1}{2}}$ must be divided by k before the core is selected.

Finally it must be remembered that transformers which are designed to transmit powers of the order of 1kW tend to be wound with rather heavy conductors. At frequencies of more than a few kHz eddy current effects in the winding can raise the winding resistance by a large factor and the foregoing analyses and procedures are invalidated. When eddy currents are likely to be present it is far more difficult to select a core. These problems are discussed later.

Example design of a low frequency power transformer

To illustrate the application of ferrite cores to a practical transformer the following specification will be used as an example:

Output power	1kW at 1kHz
Primary voltage	1kV
Secondary voltage	200V at full load
Regulation	<5%

Nominal cooling conditions will be assumed. Reference to Fig. 10 shows the design falls in the saturation limited class and that cores SLE3 and SSE4 should both be suitable. As the former has a slightly smaller volume it will be used for this design. The properties of core SLE3, taken from Table 3 are:

Core cross-sectional area $A_e = 1350\text{mm}^2$
Effective volume $V_e = 307\times10^3\text{mm}^3$
Core factor $C_1 = 0{\cdot}168\text{mm}^{-1}$
Window width $b_a = 60\text{mm}$
Window height $h_a = 30\text{mm}$
Window area $A_a = 1800\text{mm}^2$
Mean turn length $l_w = 244\text{mm}$
Nominal total loss $P_{tot} = 16{\cdot}2$
(corresponding to 300μW.mm^{-2})

The maximum flux density is taken as 0·3T (3000Gs) as this was the value assumed in deriving the curves in Fig. 10. From Eq. 11 the number of primary turns,

$$N_1 = \frac{\surd 2\times1000}{2\pi10^3\times0{\cdot}3\times1350\times10^{-6}} = 556 \text{ turns.}$$

Therefore

$$N_2 = 111 \text{ turns (uncorrected for regulation).}$$

The net winding breadth will be taken as 50mm and the net winding height, after allowing for a coil former, bowing of the winding, etc., will be taken as 22mm. The net winding area, $A_w = 22\times50 = 1100\text{mm}^2$. Thus the approximate cross-sectional area available for each winding is 550mm^2.

An approximate value of the primary overall conductor diameter may be obtained from:

$$d_o \approx \sqrt{\frac{550}{556}} = 0{\cdot}994\text{mm.}$$

This ignores the presence of interleaving insulation and so a somewhat smaller conductor diameter must be used in practice.

If medium covered enamelled copper wire is used, a suitable conductor diameter is d = 0·813mm (0·032in). This has a maximum overall diameter of 0·8966mm. Allowing a factor of 0·95 for the residual spacing between turns in a closely wound layer, the number of turns per layer is given by

$$\frac{50\times0{\cdot}95}{0{\cdot}8966} = 53.$$

Therefore

$$\text{number of layers} = \frac{556}{53} \approx 10{\cdot}5 \text{ (or 11 rounded to the next higher integer).}$$

The actual height occupied by this winding may be estimated as 11 (0·8966+t)mm where t is the thickness of the layer interleaving material. Assuming t = 0·1mm the primary winding height will be 11mm.

The corresponding calculation for the secondary is as follows. Approximate overall conductor diameter, $d_o \approx (550/111)^{\frac{1}{2}} = 2{\cdot}23$mm. A suitable conductor diameter would be d = 1·83mm (0·072in). This has a maximum overall diameter of 1·943mm. The maximum number of turns per layer is 50×0·95/1·943 = 24·4 and the number of layers is 111/24·4 = 4·55. The actual winding height of the secondary, allowing for 0·2mm interleaving, is 5(1·943+0·2) = 10·7mm.

Allowing an extra 0·3mm for the insulation and, if required, a screen between the windings, the total winding height is 22mm. This is exactly equal to the maximum winding height assumed at the outset so it must be expected that the winding will be rather full. If a more generous margin is considered desirable the conductors of each winding may be reduced by one gauge. However, with heavy conductors the difference between adjacent standard diameters is rather large and it is often difficult to achieve well-balanced winding resistances within the height and winding resistance limitations.

If the mean turn length, 244mm, is taken to apply to both windings, the winding resistances are

Primary: 556×0·03265×0·244 = 4·43Ω
Secondary: 111×0·006449×0·244 = 0·175Ω

The second figure in each multiplication is the resistance of the conductor in ohms per metre. These figures are the room temperature values and are used for convenience. In a practical design the resistances at the working temperature would be calculated using the temperature coefficient of the resistivity, or more conveniently multiplying the 20°C values by the factor m (see the caption of Table 3). The errors introduced by taking the mean turn length to apply to each winding individually tend to cancel when the total winding resistance or loss is considered.

The total power loss:

Primary winding loss: $I^2R = 1\times4{\cdot}43 = 4{\cdot}43\text{W}$
Secondary winding loss: $= 25\times0{\cdot}175 = 4{\cdot}38\text{W}$
Core loss: $w_mV_ef = 18\times10^{-9}\times307\times10^3\times10^3 = 5{\cdot}53\text{W}$

where w_m is the core loss density per cycle and has been assumed to be
18×10^{-9} J.mm^{-3}.cycle^{-1}.as in Fig. 10

Total 14·34W

This compares with a nominal total loss, P_{tot}, of 16·2W, thus the transformer will be operating inside its nominal rating. It is interesting to note that the nominal total copper area of the primary is 288mm^2 and, of the secondary, 292mm^2. The sum of these copper areas divided by the total window area, A_a, 1800mm^2, gives an overall copper factor, F_a, of 0·321. This compares with 0·30 assumed in compiling Table 3 and Fig. 10. The rather high value is due to the very full winding that has been fortuitously obtained and it accounts for the total loss being less than the nominal value.

The full load voltage drop in the winding resistance referred to the secondary side is

$$I_2(R_2+R_1/r^2) = 5(0{\cdot}175+4{\cdot}43/25) = 1{\cdot}76\text{V.}$$

where r is the turns ratio.

This voltage is less than 1% of the open circuit secondary voltage and there is no need for turns adjustment on this account.

It remains to check the voltage drop due to leakage inductance.

This has been calculated using the conventional formula, for example, see Ref. 8, and the value obtained is $L_\ell =$ 570μH.

The voltage drop across this reactance is $I_2\omega L_\ell = 5\times2\pi\times10^3\times570\times10^{-6} \approx 18$V. The output voltage at full load, ignoring winding resistance and assuming an induced e.m.f. of 200V, is $\surd(200^2-18^2) \approx 199{\cdot}2$V. Thus the voltage drop at full load due to the leakage inductance is 0·8V which is also negligible. Had it been outside the limit so that a correction would have been required, it would be normal practice to increase the number of secondary turns to give the nominal output voltage at full load. If such adjustment is likely to be required it is an advantage for the secondary winding to have an incomplete last layer so that the extra turns may be easily accommodated. On the other hand if the leakage inductance were excessive it could be reduced by sandwiching the secondary between two sections of the primary, one above and one beneath.

Finally the magnetizing current may be checked. Assuming that the effective permeability of the core is 1000, the primary shunt inductance is

$$L_p = \frac{\mu_o\mu_eN^2}{C_1} = \frac{4\pi\times10^{-7}\times10^3\times556^2}{0{\cdot}168\times10^3}.$$
$$= 2{\cdot}31\text{H.}$$

Therefore the magnetizing current is

$$U_1/\omega L_p = 10^3/6{\cdot}28\times10^3\times2{\cdot}31 = 0{\cdot}069\text{A}$$

which is quite satisfactory in relation to the primary full load current of 1A.

This example illustrates the design procedure for a low frequency, saturation limited, power transformer. Had the design been loss limited the main difference would have been in the core selection. This would have been made in accordance with the procedure given earlier and then the design would have proceeded as in this example, the core loss being calculated from $(R_p)_1$ obtained from Fig. 7.

HIGHER FREQUENCY POWER TRANSFORMERS

General

The power transformers discussed in this section are those in which eddy current considerations influence the design or performance of the windings. The actual frequency at which this occurs depends on the circumstances; for example, a transformer designed to deliver 1kW into 10Ω will have such thick conductors that the a.c. resistance may be as much as five times the d.c. resistance at frequencies as low as a few kilohertz, while on the other hand a transformer delivering relatively little power into a high impedance load might have negligible winding loss at several hundred kilohertz. In low power wideband transformers the attenuation limits the winding resistance but in power transformers it is more often the heat dissipation that is the limiting factor. Thus the higher the transmitted power the more important is the effect of eddy currents; high power implies high currents, and heavy conductors imply relatively high a.c. resistance due to eddy currents.

The design procedures for higher frequency power transformers are complicated by these eddy current losses in the windings. The methods of core selection described in the foregoing sections no longer apply and to some extent it is necessary to resort to trial and error methods. However a number of guiding principles are available to the designer. These will be discussed in the following sections.

Given proper data, the core performance is readily predictable but the winding gives rise to losses, leakage inductance and self capacitance all of which must be within limits if the transformer performance is to be satisfactory. Thus the optimum winding geometry usually presents the major problem in the design of a high frequency transformer.

Another general problem is cooling. If the transmitted power is large there will be an appreciable amount of power converted to heat. It is often impracticable to make the transformer large enough to dissipate this heat at a safe temperature by natural air convection; to meet leakage inductance and self capacitance specifications it is usually necessary to restrict the size. It follows, therefore, that more effective cooling methods, for example, oil cooling, are usually used for h.f. high power transformers; the rate of heat transfer is a major design parameter.

Core selection

The majority of transformers operating in the higher frequency range will be core loss limited in the design. Possible exceptions are wideband transformers that have to meet a severe attenuation or return loss specification at the lower end of the transmission band; in such cases the shunt inductance may determine the number of turns.

The higher frequency range has been defined as that in which eddy currents influence the winding design or performance. At the lower end of this range the transformers will not be very different in application or appearance to the low frequency transformers considered earlier in this article. They will probably be single frequency or narrow band devices, they will have windings that occupy a large proportion of the available winding space and the total cooling area will be approximately as expressed by A_c in Table 3. Under these circumstances the discussion of low frequency transformers given earlier is relevant.

Previous designs or other considerations may suggest that a particular core should be used. Where such guidance is not available it is inevitable that some guesses will have to be made. A guess may be made in choosing a probable core for a trial design, the first in a series of successive approximations. The alternative is to make a guess concerning the effect of eddy currents on the winding resistance. Basic data for estimating the a.c. winding resistance are given in Ref. 8. For a given winding it is possible to calculate a factor, F_R, by which the a.c. resistance exceeds the d.c. value. It depends on the conductor diameter, the geometry of the winding and the frequency; it may vary widely from one design to another. Some guiding considerations are discussed in the next section and from these it may be possible to guess a value for F_R. This may be included in Eq. 27:

$$\frac{P_o}{\sqrt{[F_a(R_p)_1]}} = \frac{P_{to}t}{4}\sqrt{\frac{A_aA_e}{\rho_cl_wl_eF_R}} = \frac{k_2}{\sqrt{F_R}} .$$

As this method provides only a rough guide the factor m has for convenience been put equal to unity.

$$P_o\sqrt{\frac{F_R}{F_a(R_p)_1}} = k_2 \quad W.\Omega.^{-\frac{1}{2}}m^{\frac{1}{2}} \quad . \quad \ldots(28)$$

If it is possible to make a reasonable guess for the ratio F_R/F_a the method of core selection becomes the same as that described earlier, that is, a core is chosen that has a value of k_2 that is equal to or greater than the value calculated by Eq. 28, using Fig. 8 to estimate the value of $(R_p)_1$. The a.c. resistance factor has been coupled with the copper factor, F_a, because they both depend on the winding geometry. If the winding fills the available space so that $F_a \approx 0{\cdot}3$ as assumed for low frequency transformers, the conductor diameter may be large enough to make F_R very high (about 50). F_R may be reduced by using a smaller diameter; indeed it is shown in the next section that for least a.c. resistance F_R should be in the region of 1·5. A straightforward reduction of conductor diameter will also reduce F_a, hence the need to consider the two factors together. The use of bunched conductors to make eddy currents negligible would return the design to the low frequency category, that is $F_R \approx 1$, but the copper factor would be somewhat less than 0·3.

A core having been selected, by one means or another, the trial design may proceed. Assuming the core is listed in a table such as Table 3 the permissible dissipation may be obtained from the appropriate column or, if the average rate of heat transfer differs from 300μW.mm^{-2} (0·2W.in^{-2}), the actual rate of heat transfer must be multiplied by the total cooling area to obtain the total dissipation. Some fraction of this (for example, a half) may be allocated to the core and, from the core volume, the core loss density may be calculated. Using core loss data such as given in Fig. 6 a value of flux density may be obtained corresponding to the permissible core loss density at the operating frequency. If the transformer is to operate over a band of frequencies, this and the following steps should be made using frequencies corresponding to each end of the band so that the design may accommodate the worst case. From the frequency, flux density and terminal voltages the number of turns may be evaluated using the e.m.f. equation Eq. 11.

A trial winding design may now be made, using the recommendations of the next section as a guide to the best conductor diameter. The d.c. winding resistance may be calculated in the usual way. The factor F_R may then be calculated for each portion of the winding according to the procedure described later and the a.c. resistance of each winding may be obtained. For a wideband transformer with a maximum load current that is independent of frequency, the upper frequency limit must be used in calculating the a.c. resistances. The maximum power loss in the windings may now be calculated from the full-load currents and the a.c. winding resistances. If this is excessive, or in the wrong proportion to the core loss, a different core or winding arrangement must be used and the design process repeated until a satisfactory solution is found. If there is a minimum inductance limit, each design should be checked to ensure that this limit is not infringed. In some cases, such as wideband transformers operating at relatively low power, the inductance consideration overrides that of core loss in determining the number of turns and the design procedure approaches that described for wideband transformers.

As explained at the beginning of this section, the foregoing remarks apply to transformers designed for the lower end of the higher frequency region. Attention may now be turned to the situation at much higher frequencies. Transformers designed to operate at these higher frequencies differ appreciably in application and appearance from the previously considered low frequency transformers. They are usually required to transmit a band of frequencies, a typical bandwidth ratio being 10. They will consequently need to have low leakage inductance and low self capacitance, and so the windings will usually be designed as single layers, well spaced from the core and from each other. The cooling area will not therefore correspond to that used for low frequency transformers. To ease the problem of designing the winding to meet the high frequency specification it is necessary to restrict the size of the transformer. This usually entails a more effective means of heat transfer than free air convection; oil cooling is often used.

It follows from these considerations that h.f. power transformers tend to have an open construction in which the entire core surface can transfer heat directly to the convection medium. If this type of construction is assumed the thermal balance of the core is almost entirely isolated from that of the winding and so the design of the core may be largely independent of the winding design.

It is assumed that the frequency and core size are such that, to avoid eddy current losses in the core, the choice of ferrite must be confined to the nickel zinc grades. To avoid an excessive core loss density at high frequencies it is usually necessary to restrict the flux density to quite low values, less than, for example, 10mT (100Gs). Under these conditions the residual loss is the main component of the magnetic loss in the core. Therefore the magnetic core loss density may be related to the residual loss factor as follows:

$$P_m = \left(\frac{\tan\delta_r}{\mu}\right).\frac{\pi f\hat{B}_e{}^2}{\mu_o} \quad W.m^{-3} \quad . \quad \ldots(29)$$

The residual loss factor $(\tan\,\delta_r)/\mu$ is a function of frequency and temperature and graphical data relating to suitable materials are readily available. The ferrite with the lowest residual loss factor under the appropriate conditions will be the most suitable. Given a grade of ferrite, Eq. 29 relates the core loss density to the flux density.

In the problem of core selection the starting parameters depend to some extent on the circumstances. One approach is to start with the core temperatures and base the selection on thermal equilibrium. To establish the relevant relations, a hypothetical core having a uniform circular cross-section of diameter d and a volume V may be considered. The temperature difference between the centre and the surface of the core is designated θ_{cs}, and is related to the core loss density by Eq. 9:

$$\theta_{cs} = \frac{P_md^2}{16\lambda} \quad degC \quad . \quad \ldots(30)$$

Assuming the flux density is uniform the total power dissipated in the core is P_mV and at equilibrium this equals the total rate of heat transfer, that is

$$P_mV = P_{conv}A_c \quad W \quad \ldots(31)$$

where A_c is the surface area of the core

and P_{conv} is the heat transfer per unit area.

Combining this in Eq. 30:

$$P_{conv} = \frac{16V\lambda\theta_{cs}}{A_cd^2}$$

$$= \frac{4\lambda\theta_{cs}}{d} \quad W.m^{-2} \quad . \quad \ldots(32)$$

If d is in mm and λ for ferrite is 4000μW.mm^{-1}.deg^{-1}C:

$$P_{conv} = \frac{16\times10^3\times\theta_{cs}}{d} \quad \mu W.mm^{-2} \quad . \quad \ldots(33)$$

If thermal considerations enable the designer to decide the temperature of the core surface and the temperature of the core centre these equations enable the corresponding diameter and core loss density to be determined. The method of heat transfer and the permissible surface temperature together determine the rate of heat transfer P_{conv} (see, for example, Fig. 3). The difference between the surface and centre temperatures equals θ_{cs}. Thus Eq. 33 yields d and Eq. 30 yields P_m and hence the flux density.

These parameters are not dependent on the total power to be transmitted because the only design criterion was temperature distribution. If the transformer is required to transmit a band of frequencies, the flux density calculation must be made at several frequencies within the band so that when the corresponding numbers of turns are subsequently calculated the limiting case (that yielding the largest number of turns) may be determined.

It is interesting to note that if, for the purpose of facilitating the h.f. aspects of the design, it is desired to minimize the length of the winding conductor then it is necessary to minimize πdN

or $d/\hat{B}A$ (from Eq. 11),

that is, maximize $\hat{B}d$ (since $A = \pi d^2/4$)

or $\sqrt{P_m}.d$ (since $P_m \propto \hat{B}^2$ approx.)

Applying this to Eq. 30 it is clear that θ_{cs} should be made as high as thermal considerations will allow.

From the e.m.f. equation, the number of turns may be calculated and the subsequent winding design will determine the winding breadth required. The cross-sectional area and the winding breadth having been determined, a suitable core may be selected. In practice a uniform cylindrical core will not normally be available and the selection will probably be made from a standard range having rectangular cross-sections, such as the range shown in Table 3. Under these circumstances the core diameter, d, must be replaced by an effective cross-sectional dimension. Such values have been listed in Table 3 under the designation d_e. When the core has a double E shape the centre leg is the limb that will reach the highest temperature and therefore where appropriate d_e refers to this limb.

The above approach will lead to the selection of a suitable core provided the design is core loss limited. This is not always true; if the bandwidth is wide the minimum shunt inductance will determine the number of turns. Therefore when the core has been selected on magnetic loss considerations and the corresponding number of turns has been calculated, the shunt inductance must be checked. If it is found that the inductance is insufficient to meet the attenuation or return loss specification a number of courses are open. It would, for example, be possible simply to increase the number of turns but this would probably make it more difficult to meet the leakage inductance and self capacitance requirements, and since it would lower the flux density it would result in the core being operated at temperatures lower than the permitted values. A better course is to repeat the design on a ferrite having a higher permeability. This will probably have a higher value of loss factor $(\tan\,\delta_r)/\mu$ so the design approach starting from core temperatures will, in fact, result in a higher number of turns.

However, the number of turns required to obtain the specified inductance will be less than for the previous design because the permeability is higher. In principle it would be possible to balance the design so that the specified

---

(Eq. 29) $P_m = \left(\frac{\tan\delta_r}{\mu}\right)\frac{fB_e{}^2 10^{-7}}{4}$ W.cm^{-3}.

inductance and the specified core temperatures were simultaneously achieved, giving the most economical use of the core material.

If it is difficult to obtain sufficient heat transfer from the core, cooling ducts may be provided. When the core is made from units such as the U cores in Table 3 cooling ducts may easily be provided by spacing the units. For oil cooling the spacing should not be less than 3mm.

So far all the core loss has been assumed as magnetic in origin. Where there are high frequency, high voltage terminals adjacent to the ferrite the intense electric fields can give rise to high dielectric losses in the core. The resultant local heating may fracture the ferrite. The remedy is to screen those parts of the core that are exposed to intense h.f. electric fields. The screens should be applied in such a way as to avoid excessive interception of the magnetic fields; thus, a cylindrical core might be covered by an earthed screen which is divided into narrow strips parallel to the axis. In the application of such screens the cooling of the core must not be impeded and the clearance to the winding must be adequate to prevent excessive capacitance or the chance of voltage breakdown.

Summarising the problem of core selection for the higher frequency transformer, the temperature limitations will narrow the choice to cores of particular cross sectional dimensions (d_c in Table 3) and the inductance considerations may in addition determine the core factor C_1. The final selection will depend on the winding; in particular the core must provide sufficient winding breadth. Some of the aspects of winding design will be considered in the next section.

Windings

In the context of this article the higher frequency range is defined as that in which copper eddy currents influence the winding design. As in the previous section the problem may be considered in two parts, starting with transformers for the lower frequency end of this range. In such transformers the windings will normally occupy an appreciable proportion of the winding space and usually an attempt will be made to relate the core and winding losses. The presence of eddy currents makes it difficult to estimate the latter in advance. The way in which this difficulty influences the choice of a core was considered at the beginning of the previous section. Assuming that a core has been selected for an initial design, the problem is to design the winding for minimum loss. Before considering this problem analytically it is instructive to apply the method given in the Appendix to a given winding. For the purpose of illustration the example transformer design worked out in an earlier section will be used and the a.c. resistance of the windings at an arbitary frequency of 5kHz will be calculated.

The simple winding arrangement shown in Fig. 12(*a*) will be assumed, so that each complete winding constitutes one winding portion. For each portion it is necessary to obtain the number of turns per layer, N_ℓ, the effective conductor height, h, the layer copper factor, F_ℓ, and the number of layers, p.

Considering the primary winding first, this consists of 556 turns of 0·813mm (0·032in) diameter copper wire. From the earlier calculation $N_\ell = 53$, $p = 11$, and the d.c. resistance is 4·43Ω. From Fig. 13, $h = 0{\cdot}886 \times 0{\cdot}813 = 0{\cdot}72$mm and from Eq. 45 $F_\ell = 53 \times 0{\cdot}72/50 = 0{\cdot}76$.

From Table 4, the penetration depth, Δ, for copper at 5kHz and 20°C is 0·925mm (in a practical design the value of Δ would correspond to the working temperature). Thus the value of the variable in Fig. 14 is

$$\frac{h\sqrt{F_\ell}}{\Delta} = \frac{0{\cdot}72\sqrt{0{\cdot}76}}{0{\cdot}925} = 0{\cdot}68 \quad .$$

From Fig. 14, putting $p = 11$, the value of F_R is about 3·9 so the a.c. resistance of the primary is $3{\cdot}9 \times 4{\cdot}43 = 17\Omega$.

Similarly for the secondary,

$$N_\ell = 24{\cdot}4 \qquad p = 5 \qquad R_{dc} = 0{\cdot}175\Omega$$

$$h = 1{\cdot}62 \qquad F_\ell = 0{\cdot}79$$

Therefore

$$\frac{h\sqrt{F_\ell}}{\Delta} = 1{\cdot}56.$$

$$F_R = 13,$$

and the a.c. resistance of the secondary is $13 \times 0{\cdot}175 = 2{\cdot}3\Omega$. It should be noted that in the earlier d.c. resistance calculation the mean turn length was assumed to be the same for both windings. For the simple arrangement where one winding is wound over the other this assumption leads to one winding resistance being lower than calculated and the other being higher. In the summation the error is cancelled. But when calculating the a.c. resistance, each d.c. winding resistance is in general increased by a different factor F_R and this can lead to error if the mean turn lengths for the two windings are significantly different. In such a case the mean turn length should be calculated for each winding; in the foregoing example this has been ignored for the sake of simplicity.

This example demonstrates that the eddy current loss in heavy gauge windings can be appreciable even at quite low frequencies. In this particular case considerable improvement could be obtained by changing the winding configuration to that shown in Fig. 12(*b*).

The problem of choosing the optimum conductor cross-section will now be considered analytically, extending Dowell's results (Ref. 10) in the Appendix. First it is necessary to emphasize the significance of the parameter p. This is the number of layers in a winding portion as defined in the Appendix. A winding portion is that part between the surface of a winding and the surface of zero m.m.f. (see Fig. 12). This may include the whole winding as in Fig. 12(*a*) or it may be half a winding as in the primary winding of Fig. 12(*b*). Thus a winding portion for which $p = 2{\cdot}5$ will be half a 5-layer winding, that is, it will occupy a winding height equal to 2·5 times the layer thickness. In all cases the layers are assumed to be complete: indeed incomplete layers invalidate the theory and should be avoided as they will give rise to excessive eddy current losses when only a few layers are used. Although the derivation involves a layer copper factor, F_ℓ (see Eq. 45), if this becomes too small, that is, with turns too widely spaced, the theory becomes unreliable.

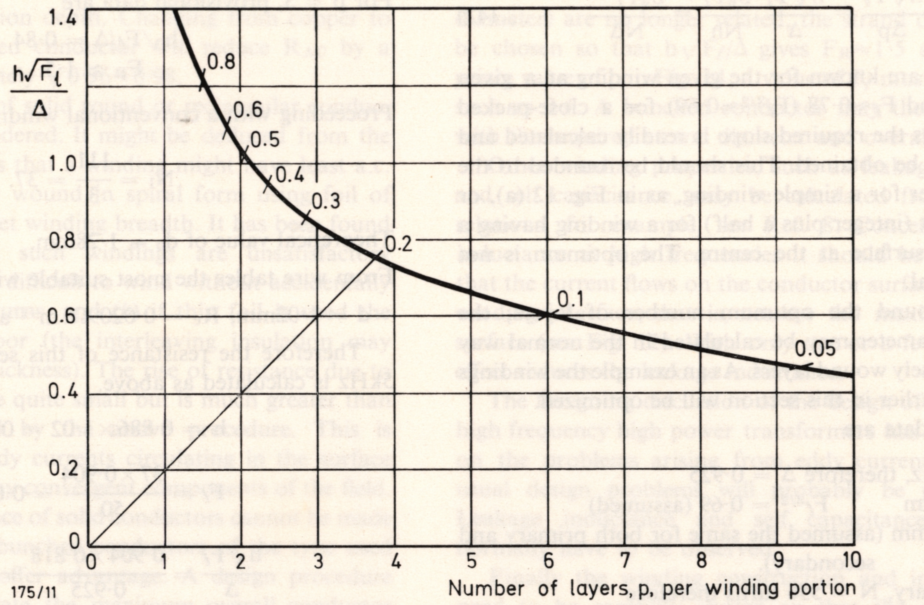

Fig. 11—$h\sqrt{F_\ell}/\Delta$ as a function of p for minimum high frequency resistance of a close packed winding of round wire. The marks are the intersects of the curve with straight lines from the origin having the indicated slope; the slope $= b_w F_\ell^{3/2}/N\Delta$. The latter function is calculable from given data; its intersection with the curve gives the optimum values of $h\sqrt{F_\ell}/\Delta$ and p

The most interesting case is the close-packed multi-layer winding of N turns occupying a winding breadth b_w. Assuming solid round wire is to be used the problem is to determine the wire diameter that will give minimum a.c. resistance. Reference to Fig. 14 shows that each curve starts at the lower end by an upward curvature, then there is a steep straight portion and this is followed by a straight portion in which $F_R \propto h\sqrt{F_\ell}/\Delta$ (in the present context $h = 0{\cdot}886 \times$ copper dia.).

The a.c. resistance of the winding is $F_R R_{dc}$. For the close packed winding under consideration it may be seen from the Appendix that

$$R_{dc} \propto \frac{1}{h^2} \quad . \qquad \ldots(34)$$

It follows that in the upper straight region of the curves

$$R_{AC} = F_R R_{dc} \propto \frac{1}{h} \qquad \ldots(35)$$

so the largest possible conductor should be used. However when $h\sqrt{F_\ell}/\Delta$ is less than about 2 a different situation occurs. It is clear that the steepness of the curve will cause $F_R R_{dc}$ to be a minimum towards the lower curved region. In this region Dowell's expression for the curve may be approximated to

$$F_R = 1 + \frac{1}{45}(5p^2-1)\left[\frac{h\sqrt{F_\ell}}{\Delta}\right]^4 . \qquad \ldots(36)$$

Therefore

$$R_{AC} \propto \frac{1}{h^2}\left\{1 + \frac{1}{45}(5p^2-1)\left[\frac{h\sqrt{F_\ell}}{\Delta}\right]^4\right\} \qquad \ldots(37)$$

Now $Fl = \frac{N_1 h}{b_w}$(see Eq. 45).

Therefore

$$p = \frac{N}{N_\ell} = \frac{Nh}{b_w F_\ell} . \qquad \ldots(38)$$

Therefore

$$R_{AC} \propto \frac{1}{h^2} + \frac{N^2h^4}{9b_w{}^2\Delta^4} - \frac{h^2F^2{}_\ell}{45\Delta^4} . \qquad \ldots(39)$$

Differentiating this expression with respect to h and equating to zero, R_{AC} is minimum when

$$\left[\frac{h\sqrt{F_1}}{\Delta}\right]^4 = \frac{45}{10p^2-1} \quad . \qquad \ldots(40)$$

If this is substituted in Eq. 36

$$\left.\begin{aligned} F_R &= 1 + \frac{5p^2-1}{10p^2-1} \\ &\rightarrow 1{\cdot}5 \text{ when } p > 1 \end{aligned}\right\} \qquad \ldots(41)$$

Thus as a general rule, when the conductor diameter cannot be so large that $d/\Delta \geqslant 2$, the diameter should be such that $F_R \approx 1{\cdot}5$. To find the optimum diameter, the values of h and p must be found that simultaneously satisfy Eqs. 38 and 40. The latter equation is plotted in Fig. 11 and the points are marked where the curve intersects with straight lines from the origin having various values of slope.

The slope of these lines from Eq. 38 is

$$\frac{h\sqrt{F_\ell}}{\Delta p} = \frac{h\sqrt{F_\ell}}{\Delta} \cdot \frac{b_w F_\ell}{Nh} = \frac{b_w F_\ell^{3/2}}{N\Delta} \qquad \ldots(42)$$

N, b_w and Δ are known for the given winding at a given frequency, and $F_\ell \approx 0{\cdot}78$ ($F_\ell^{3/2} \approx 0{\cdot}69$) for a close-packed winding. Thus the required slope is readily calculated and hence p may be obtained. This should be rounded to the nearest integer for a simple winding, as in Fig. 12 (a), or to the nearest (integer plus a half) for a winding having a zero m.m.f. surface at the centre. The optimum is not usually critical.

Having found the optimum number of layers, the conductor diameter may be calculated in the normal way assuming closely wound layers. As an example the windings considered earlier in this section will be optimized.
The starting data are

$$f = 5\text{kHz, therefore } \Delta = 0{\cdot}925$$
$$b_w = 50\text{mm} \qquad F_\ell^{3/2} = 0{\cdot}69 \text{ (assumed)}$$
$$l_w = 244\text{mm (assumed the same for both primary and secondary).}$$

For the primary, N = 556 turns therefore

$$\frac{b_w F_\ell^{3/2}}{N\Delta} = \frac{50 \times 0{\cdot}69}{556 \times 0{\cdot}925} = 0{\cdot}067.$$

Constructing a line having a slope of 0·067 on Fig. 11, it intersects the curve at p = 7·6. Using p = 8 the data yields the following provisional values: $h\sqrt{F_\ell}\Delta = 0{\cdot}52$ and $F_R = 1{\cdot}5$.

Making a conventional winding design with p = 8:

$$N_\ell = \frac{556}{8} \approx 69{\cdot}5.$$

Therefore the theoretical overall conductor diameter allowing a layer packing factor of 0·95 is given by

$$d_o = \frac{50 \times 0{\cdot}95}{69{\cdot}5} = 0{\cdot}684\text{mm}.$$

The nearest suitable wire has a copper diameter, d = 0·61mm; the resistance, R_c, is $0{\cdot}05804\Omega.\text{m}^{-1}$ and the diameter of medium enamelled covering is 0·686mm. The resistance of this practical winding at 5kHz may now be calculated as before:

$$h = 0{\cdot}886 \times 0{\cdot}61 = 0{\cdot}540\text{mm}$$
$$F_\ell = 69{\cdot}5 \times 0{\cdot}540/50 = 0{\cdot}751$$
$$\frac{h\sqrt{F_\ell}}{\Delta} = \frac{0{\cdot}540 \times 0{\cdot}867}{0{\cdot}925} \approx 0{\cdot}51.$$

From Fig. 14, $F_R \approx 1{\cdot}5$.
The d.c. resistance $= N.R_c.l_w = 556 \times 0{\cdot}05804 \times 0{\cdot}244 = = 7{\cdot}87\Omega$.
Therefore $R_{AC} = 1{\cdot}5 \times 7{\cdot}87 = 11{\cdot}8\Omega$.
This compares with 15·9 for the previous design, which used the largest possible wire diameter.

The corresponding calculation for the secondary is:

$$N = 111 \text{ turns.}$$
$$\frac{b_w F_\ell^{3/2}}{N\Delta} = \frac{50 \times 0{\cdot}69}{111 \times 0{\cdot}925} = 0{\cdot}336.$$

From Fig. 11 $p \approx 2{\cdot}7$.
For p = 3, provisional data are

$$h\sqrt{F_\ell}/\Delta = 0{\cdot}84$$
$$F_R \approx 1{\cdot}5.$$

Proceeding with a conventional winding design

$$N_l = \frac{111}{3} = 37.$$

Theoretical value of $d_o \approx 1{\cdot}28$mm.
From wire tables the most suitable wire has

$$d = 1{\cdot}02\text{mm}, \; R_c = 0{\cdot}0209\Omega.\text{m}^{-1} \text{ and } d_o = 1{\cdot}11\text{mm}.$$

Therefore the resistance of this secondary winding at 5kHz is calculated as above.

$$h = 0{\cdot}886 \times 1{\cdot}02 = 0{\cdot}904\text{mm}$$
$$F_\ell = \frac{37 \times 0{\cdot}904}{50} = 0{\cdot}669$$
$$\frac{h\sqrt{F_\ell}}{\Delta} = \frac{0{\cdot}904 \times 0{\cdot}818}{0{\cdot}925} = 0{\cdot}80.$$

From Fig. 14 $F_R \approx 1{\cdot}45$.
The d.c. resistance is $111 \times 0{\cdot}0209 \times 0{\cdot}244 = 0{\cdot}566\Omega$, therefore

$$R_{AC} = 1{\cdot}45 \times 0{\cdot}566 = 0{\cdot}821\Omega.$$

This compares with 2·1Ω for the previous design.

Returning to the general case, if the indicated number of layers approaches unity a different situation exists. Because a partly filled layer is inadmissible the design must be based on one full layer, that is p = 1 or, if the zero m.m.f. surface divides the winding, p = ½. Considering the curves for p = 1 and p = ½ in Fig. 14 it is seen that almost the whole region above the lower curvature has a slope of approximately unity. Under these conditions it has been deduced (see Eq. 35) that $R_{AC} \propto 1/h$ so if round conductor is used it should have the largest possible diameter, that is, allowing a layer packing factor of 0·95,

$$d_o = \frac{0{\cdot}95 b_w}{N}. \qquad \ldots(43)$$

If the single layer is to consist of a conductor having rectangular cross-section, b×h (see Fig. 13), then $R_{dc} \propto 1/bh$. If the unity slope part of the F_R curve applies, $R_{AC} = F_R R_{dc} \propto 1/b$. So if $h\sqrt{F_\ell}/\Delta_m$ is less than about 2 the conductor thickness h should be increased until the part of the curve having unity slope is reached; further increase has no advantage because the current flows on or near only one of the conductor surfaces.

When the current flow is confined to a surface layer of effective thickness Δ the a.c. resistance is clearly given by $\rho_c N l_w / b_m$. Substituting from the equation given with Table 4 and putting the relative permeability of the conductor equal to unity,

$$R_{AC} = \frac{Nl_w}{b}\sqrt{(\pi\mu_o\rho_c f)}\ \Omega \qquad \ldots(44)$$

(Eq. 44) $R_{AC} = \dfrac{2\pi Nl_w}{b}\sqrt{(\rho_c f 10^{-9})}\ \Omega.$

Thus $R_{AC} \propto \sqrt{\rho_c}$; a reduction of ρ_c reduces the d.c. resistance in proportion but this is partly offset by a decrease in penetration depth. Changing from copper to silver or silver plated conductor will reduce R_{AC} by a factor of approximately $\sqrt{0{\cdot}96} \approx 0{\cdot}98$.

So far windings of solid round or rectangular conductors have been considered. It might be deduced from the above considerations that a winding might have least a.c. resistance if it were wound in spiral form using foil of width equal to the net winding breadth. It has been found experimentally that such windings are unsatisfactory because (*a*) they are difficult to wind without accidentally producing shorted turns, and (*b*) if thin foil is used the copper factor is poor (the interleaving insulation may exceed the foil in thickness). The rise of resistance due to eddy currents can be quite small but is much greater than the value predicted by the above procedure. This is probably due to eddy currents circulating in the surface of the foil, induced by convergent components of the field.

If the a.c. resistance of solid conductors cannot be made small enough then bunched conductors of the type used for inductors may offer advantage. A design procedure would be to calculate the maximum overall conductor diameter from the required number of turns and the net space available for the winding portion. From this the number of layers per portion may be deduced; this will be the minimum value of p. Since p and h (the effective strand diameter) are no longer related, the strand diameter may be chosen so that $h\sqrt{F_\ell}/\Delta$ gives $F_R \approx 1{\cdot}5$ at the appropriate value of p in Fig. 14; a value of F_ℓ must be assumed, such as 0·6. A bunched conductor may then be selected with the required strand diameter and overall diameter.

Other winding properties, such as leakage inductance and self capacitance, may be calculated from the usual relations, for example, see Ref. 8. Concerning leakage inductance at high frequencies it should be remembered that the current flows on the conductor surface nearest the winding interface, that is, nearest the maximum m.m.f. surface (see Fig. 12). With only one or a few layers, this effect reduces the leakage inductance.

The foregoing discussion of the design of windings for high frequency high power transformers has concentrated on the problems arising from eddy currents. The more usual design problems will probably be present also. Leakage inductance and self capacitance limits will normally have to be observed.

Finally the winding construction and insulation will need to be carefully chosen so that the windings will adequately withstand the high frequency high voltage conditions to which they will be subjected.

REFERENCES AND BIBLIOGRAPHY

1. KING, W. J., 'The basic laws and data of heat transmission', **Mech. Engrg, 54,** 190, (Part 1), 275, (Part 2), 347, (Part 3), 410, (Part 4) and 492, (Part 5), (1932)—table 1, p. 494.
2. KING, W. J., *ibid.*, p. 351.
3. KING, W. J., *ibid.*, p. 350.
4. BLUME, L. F., BOYAJIAN, A., CAMILLI, G., LENNOX, T. C., MINNECI, S. and MONTSINGER, V. M., **Transformer engineering,** John Wiley and Sons, Inc., New York, (1951).
5. KING, W. J., (see above), p. 426.
6. KING, W. J., *ibid.*, p. 353.
7. SNELLING, E. C., 'Soft ferrites, properties and applications', Iliffe, London (1969).
8. SNELLING, E. C., *ibid.*, chap. 11.
9. MACFADYAN, K. A., **Small transformers and inductors,** Chapman and Hall Ltd, London, (1953).
10. DOWELL, P. L., 'Effects of eddy currents in transformer windings', **Proc. Instn. Elect. Engrs, 113,** 1387, (1966).

APPENDIX

Total eddy current loss in transformer windings

In a transformer the tranverse field in the winding space may be taken as being parallel to the interfaces between windings and its magnitude may be easily evaluated. This enables a general analysis to be made. Qualitatively the combination of the transverse and the conductor fields in a normal transformer causes the current density to increase towards the surface of the conductor that faces the nearest winding interface. This will result in an increase of winding resistance and also in a fall in the leakage inductance as the frequency rises. This Appendix is only concerned with the rise in resistance. The analysis leads to a factor, F_R, by which the d.c. resistance may be multiplied. This factor is a function of the winding geometry and of a ratio involving the penetration depth; the method of determining it will now be described.

In a transformer, the ampere turns due to the primary are very nearly balanced by those due to the secondary. Moving from the innermost or outermost surface of the windings, the m.m.f. increases linearly from zero until it reaches a maximum at a primary/secondary interface after which it begins to fall linearly. Fig. 12 shows some typical winding arrangements and the corresponding m.m.f. diagrams. For the purpose of the present calculation it is necessary to divide the windings into portions in which the low frequency m.m.f. varies linearly from zero. Thus in Fig. 12(*b*) the half secondaries are portions and the primary must be divided into two equal portions. In general each portion must be considered separately, but if, for example, two are identical the value of F_R calculated for one of them would apply to both.

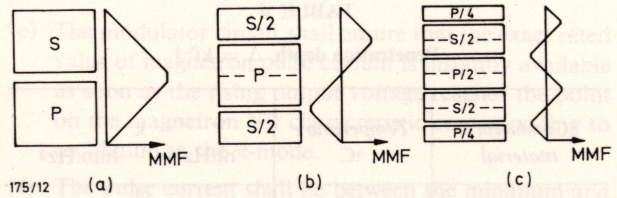

Fig. 12—Some transformer winding arrangements and the corresponding m.m.f. diagrams

For each portion the following parameters are required:

The number of turns per layer,	N_ℓ
The effective conductor height,	h
The layer copper factor,	F_ℓ
The penetration depth	Δ

Fig. 13(*a*) shows a typical layer of rectangular conductors. The layer copper factor is defined by

$$F_\ell = \frac{N_\ell b}{b_w} \qquad \ldots(45)$$

where b_w is the overall winding breadth and b is the conductor breadth. If the conductors are round, the equivalent square conductors must first be derived as in Fig. 13(*b*) and then the above parameters may be calculated, putting $h = b = 0{\cdot}886d$.

The only other information about the portion of winding that is required is the number of layers, p. In most transformers the m.m.f. diagram will be such that the number of layers will either be an integral number or, if the dividing line cuts through the middle of a layer, an integral number plus a half.

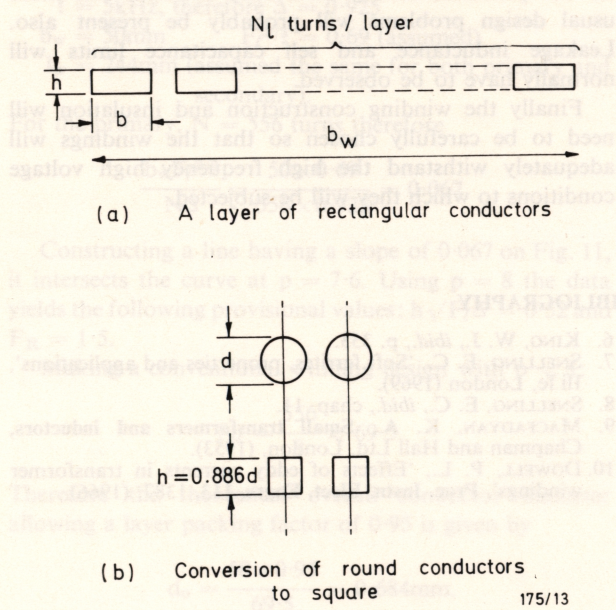
N_ℓ turns / layer
h
b
b_w
(a) A layer of rectangular conductors
d
h=0.886d
(b) Conversion of round conductors to square
175/13

Fig. 13—Winding layer parameters (note: h, b and d refer to bare conductors)

TABLE 4

Penetration depth, $\Delta = kf^{-\frac{1}{2}}$

Conductor material	*Temperature* °C	k m.Hz$^{\frac{1}{2}}$	k mm.Hz$^{\frac{1}{2}}$
Copper	20 70	0·0655 0·072	65·5 72
Aluminium	20 70	0·082 0·090	82 90
Silver	20 70	0·064 0·070	64 70

From the above parameters the variable $h\sqrt{F_\ell}/\Delta$ must be calculated; for the given frequency, Δ may be obtained from Table 4. Fig. 14 gives F_R as a function of $h\sqrt{F_\ell}/\Delta$ with the number of layers per portion as a parameter. If R_{dc} is the d.c. resistance of the portion of the winding, or of the whole winding if it has been divided into identical portions, then the corresponding resistance at the given frequency is $R_{dc}F_R$. For further details of the method and its derivation see Ref. 10.

This rapid method of estimating the a.c. resistance of transformer windings has been verified experimentally and has given reliable results over a wide range of winding configurations. However it was found to be inaccurate for windings consisting of foil extending across the whole winding width; the actual value of R_{AC} is larger than predicted, presumably because of the presence of a small component of the leakage flux perpendicular to the foil.

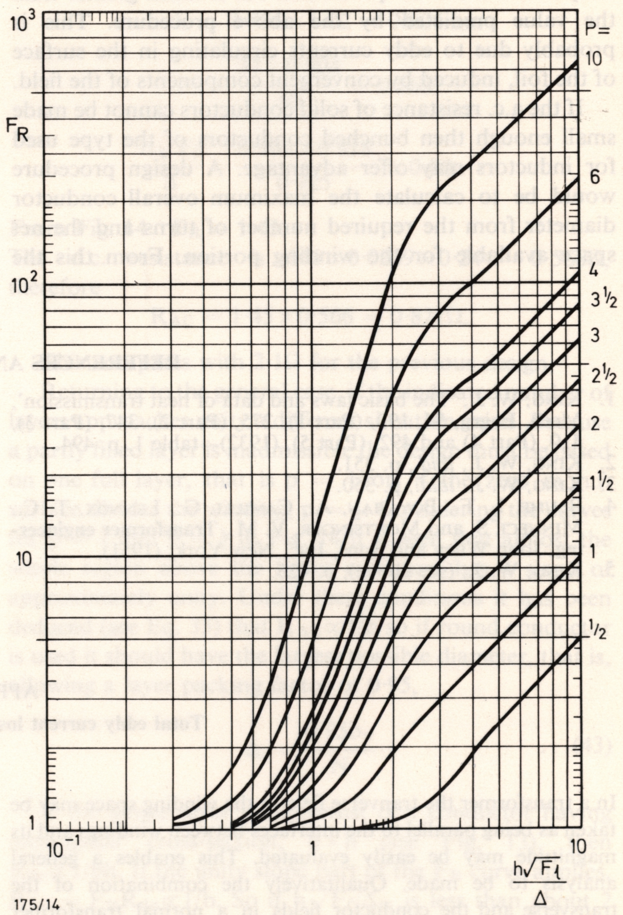

Fig. 14—F_R as a function of $h\sqrt{F\ell}/\Delta$ with number of layers, p, per winding portion as a parameter. (After Dowell (Ref. 10))

If it is found that the increase in resistance due to eddy currents is excessive, one remedy is to use bunched conductors. The permissible strand diameter may be estimated by applying the above method to the winding as if it consisted only of strands, that is, N×n turns each consisting of one strand. Then $h = 0{\cdot}886 \times$ the strand diameter, and F_ℓ is approximately equal to the net copper factor.

Pulse-modulator thyristor BTW35 as a radar magnetron driver

M. KEOHANE
Mullard Microwave Division

621.396.962.3:621.382.333.34

The BTW35 pulse-modulator thyristor may be used in a direct-switching line-type modulator to drive radar magnetrons having an r.f. pulse power output of 1 to 2kW peak. Circuit design and optimum operating conditions are discussed.

INTRODUCTION

The BTW35 thyristor is suitable for operation in simple direct-switching line-type modulators driving radar magnetrons having an r.f. pulse power output of 1 to 2kW peak; examples are the magnetrons YJ1390 and YJ1410, for which typical operating data are as follows:

TABLE 1

Typical magnetron data

		YJ1390	**YJ1410**	
Heater voltage		6·3	5·0	V
Heater current		0·4	0·72	A
Anode voltage (peak)	V_a	2·0	2·8	kV
Anode current (peak)	I_a	2·25	1·5	A
Pulse duration	t_p	0·1	1·0	µs
Pulse repetition rate		1500	2000	pulse/s
Rate-of-rise of voltage	RRV	60	17	kV/µs
Power output (peak)		1·4	1·0	kW
Frequency		9·41	5·4	GHz

Pulse amplitude (I_a), pulse duration (t_p), and rate-of-rise of voltage (RRV) are defined by joint Inter-Services Specification K1001 as follows:

1a) 'Amplitude' means the peak value of a smooth curve drawn through any ripples appearing on the top of the magnetron current pulse, and excluding any leading-edge spike whose duration is less than 10% of the pulse duration.

1b) 'Duration' means the time interval between the points at which the magnetron current is greater than 50% of the amplitude.

1c) 'Rate-of-rise of voltage' means the slope of the steepest tangent to the leading edge of the voltage pulse above 80% of the amplitude of that pulse.

Stable operation of radar magnetrons depends partly upon certain critical features of the modulator circuit design, in that

1d) The rate-of-rise of voltage shall not exceed the maximum rated value in accordance with definition (1c).

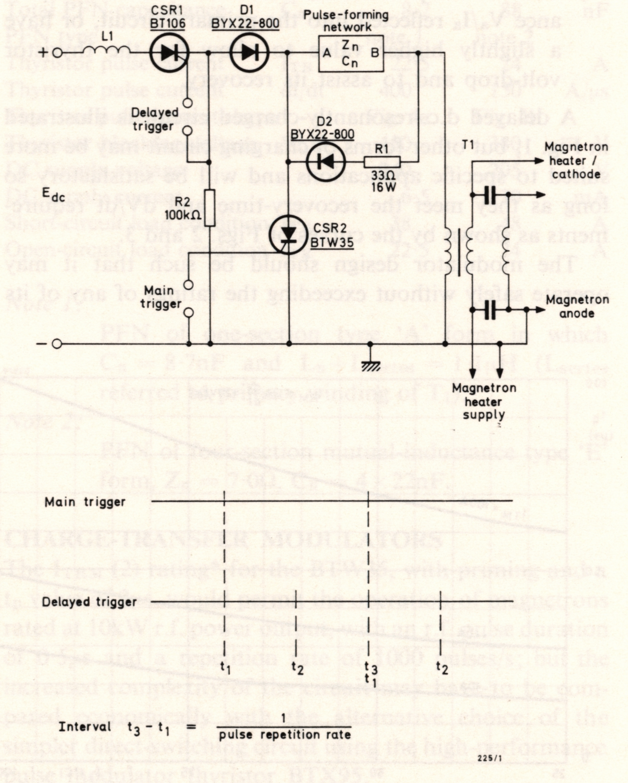

Fig. 1—Pulse-modulator circuit and pulse timing

1e) The modulator circuit shall ensure that the exact rated value of magnetron pulse current is instantly available as soon as the rising output voltage reaches the point on the magnetron V/I characteristic corresponding to oscillation in the π-mode.

1f) The pulse current shall lie between the minimum and maximum limits quoted in the operating data for the magnetron.

MODULATOR DESIGN

The circuit shown in Fig. 1 is typical of that in which the BTW35 may be used to operate the two magnetrons exemplified in Table 1, or any other magnetron requiring similar pulse input power. The requirements 1d, 1e, and 1f are met if it is ensured that:

2a) The design of the pulse transformer T_1 is such that its secondary distributed capacitance, added to that of the magnetron (typically 9pF) and any stray load capacitance, has the value:

$$C_{shunt} = I_a/RRV.$$

2b) The total effective series inductance (L_{series}) appearing between the 'line' (PFN) and the shunt capacitance C_{shunt} shall be such as to establish a value:

$$\text{Magnetron impedance}\,\frac{V_a}{I_a} = \sqrt{\frac{L_{series}}{C_{shunt}}}$$

referred to the secondary circuit. This value of L_{series} will include the leakage inductance of transformer T_1 and that of a saturable delay reactor, if used, in the primary circuit of T_1.

2c) The PFN impedance Z_n shall match the load impedance V_a/I_a reflected into the primary circuit, or have a slightly higher value to allow for the thyristor volt-drop and to assist its recovery.

A delayed d.c.-resonantly-charged circuit is illustrated in Fig. 1, but other forms of charging circuit may be more suited to specific applications and will be satisfactory so long as they meet the recovery-time and dV/dt requirements as shown by the curves of Figs. 2 and 3.

The modulator design should be such that it may operate safely without exceeding the ratings of any of its components, both whilst the magnetron is operating normally and when its output is either short-circuited or open-circuited.

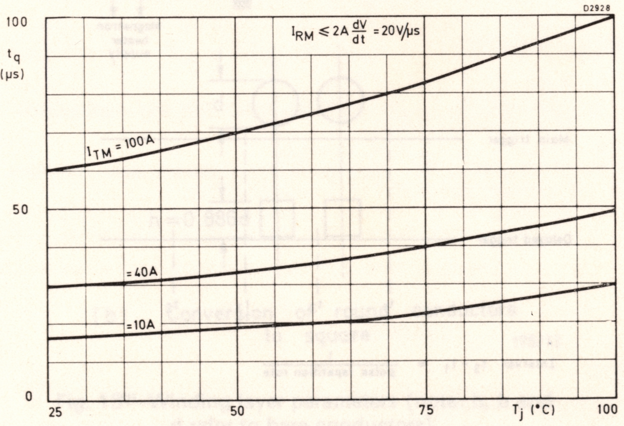

Fig. 2—Thyristor recovery time requirements

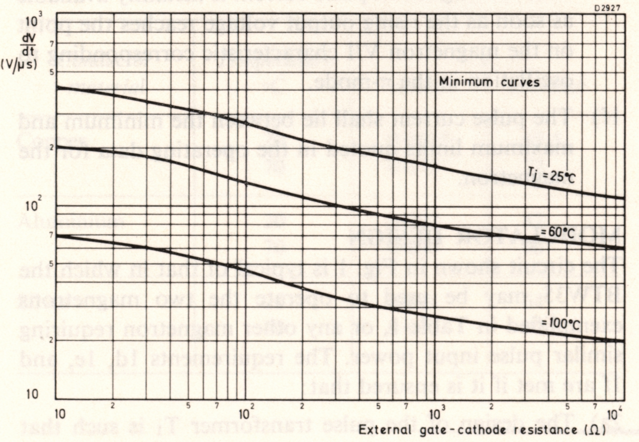

Fig. 3—Thyristor dV/dt requirements

Assurance of the requirements 2a, 2b, and 2c results in a magnetron current-pulse having an optimum leading-edge, in the correct rate-of-rise of voltage, and in good stability and shape of the r.f. spectrum from the magnetron. It also permits the thyristor circuit conditions to be determined, as outlined in the next section.

THYRISTOR CIRCUIT CONDITIONS

If the magnetron is operating normally and it is assumed that the PFN impedance has the value:

$$Z_n = V_a/(n^2 I_a)\ \ (\Omega)$$

then

$$\text{Total PFN capacitance } C_n = \frac{kt_p}{2Z_n} + \frac{n^2 I_a}{4RRV} \qquad \text{(F)}$$

$$\text{Thyristor pulse current } I_{TR} = nI_a \qquad \text{(A)}$$

$$\text{Thyristor current application } di/dt = \frac{nI_a RRV}{V_a} \qquad \text{(A/s)}$$

in which

V_a = magnetron anode pulse voltage (V)

I_a = magnetron anode pulse current (A)

t_p = magnetron current pulse duration (s)

n = pulse transformer T_1 turns ratio

RRV = magnetron voltage rate-of-rise (V/s)

k = a factor that has a value typically between 1·0 and 1·5 and allows for the measurement definition (1b) of pulse-duration at 50% amplitude, in terms of a pulse having a vertical leading edge, whilst the tail is usually cosinusoidal. The factor k is about 1·48 for a one-section network, decreasing toward unity as the number of sections is increased.

Because of the requirement to charge C_{shunt} to the magnetron threshold voltage before magnetron current starts, the current pulse I_{TR} is of longer duration than that of the magnetron current.

The forward blocking voltage V_{DW} will be equal to the charged PFN voltage E_n, and generally somewhat higher than a value:

$$V_{DW} = 2V_a/n \qquad \text{(V)}$$

because of the dynamic forward voltage $V_{T(on)}$ of the thyristor (see BTW35 data sheet).

The reapplication rate of V_{DW} is controlled by the charging inductor L_1 (Fig. 1) in association with the PFN capacitance C_n, such that

$$\frac{dV}{dt}\text{(peak)} = \frac{E_{dc}}{\sqrt{(L_1 C_n)}}. \qquad \text{(V/s)}$$

and the time interval between main and delayed trigger pulses (Fig. 1, t_1 to t_2) must allow for the requirements of Fig. 2. Hence the value of L_1 must be such as to permit the recharging of C_n to be complete within the interval t_2 to t_3, whilst not exceeding the dV/dt limits of Fig. 3, and with due allowance for the turn-off time of the charging thyristor CSR_1. The period required for recharging C_n has the value:

$$T_{charge} = \pi\sqrt{(L_1 C_n)} \qquad \text{(s)}$$

The hold-off diode D_1 is essential in addition to thyristor CSR_1; its omission may result in premature turn-on of CSR_1 due to very high values of dV/dt which occur when the modulator thyristor CSR_2 is triggered.

The inverse diode D_2 and its limiting resistor R_1 perform the usual function of discharging the capacitance C_n if the charge becomes reversed as the result of a load mismatch or short-circuit. The circuit parameters are chosen to afford protection against excessive turn-off transient power in the modulator thyristor, which may damage this device under short-circuit load conditions. Provided that the diode D_2 can handle peak currents similar to those experienced by the modulator thyristor, and the resistor R_1 can dissipate the full mean input power to the modulator, the circuit will operate safely with the magnetron short-circuited. Operation under open-circuit conditions requires that the pulse-transformer secondary-winding and connections must withstand a pulse voltage of two to three times the normal operating voltage.

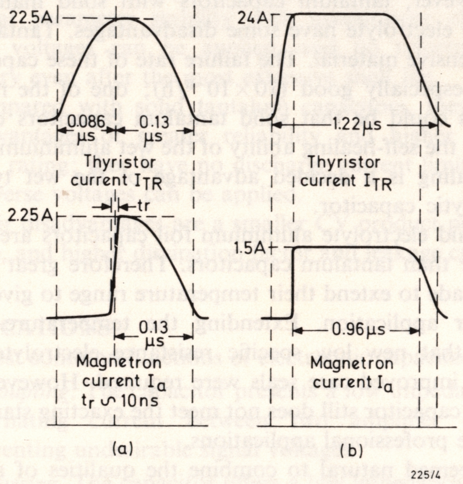

Fig. 4a—Current pulse for driving YJ1390

Fig. 4b—Current pulse for driving YJ1410

CIRCUIT VALUES AND CONDITIONS

For the Fig. 1 circuit, typical values and conditions associated with the two magnetron examples given are shown in Table 1.

TABLE 2

Circuit values and conditions

		YJ1390	**YJ1410**	
Shunt capacitance (referred to T_1 secondary)		40	88	pF
Series inductance (referred to T_1 secondary)		32·5	310	μH
Pulse transformer T_1 ratio	n	1:10	1:16	
PFN impedance	Z_n	9·5	7·0	Ω
Total PFN capacitance	C_n	8·7	88	nF
PFN type		note 1	note 2	
Thyristor pulse current	I_{TR}	22·5	24	A
Thyristor pulse current	di/dt	400	150	A/μs
Thyristor pulse current shape		Fig. 4a	Fig. 4b	
Thyristor blocking voltage	V_{DW}	450	380	V
DC supply voltage		240	205	V
DC supply current		6·5	70	mA
Short-circuit load condition	I_{TR}	38	48	A
Open-circuit load condition	I_{TR}	22·5	24	A

Note 1:

PFN of one-section type 'A' form in which $C_n = 8{\cdot}7\text{nF}$ and $L_n + L_{series} = 1{\cdot}1\mu\text{H}$ (L_{series} referred to primary winding of T_1).

Note 2:

PFN of four-section mutual-inductance type 'E' form, $Z_n = 7{\cdot}0\Omega$, $C_n = 4\times22\text{nF}$.

CHARGE-TRANSFER MODULATORS

The I_{TRM} (2) rating* for the BTW35, with priming and a t_p value of 2μs, would permit the operation of magnetrons rated at 10kW r.f. power output, with an r.f. pulse duration of 0·5μs and a repetition rate of 1000 pulses/s; but the increased complexity of the circuit may have to be compared economically with the alternative choice of the simpler direct-switching circuit using the high-performance pulse modulator thyristor BTX95.

---

* I_{TRM}=100A max for half sinewave up to 1μs, or with 5A priming for 0·25μs up to t_p=5μs.

Mullard Technical Communications
Vol. 11, No. 109, January 1971.

The article on 30mm camera tubes published in the above issue was an adaptation of material from several sources. It was only in part based on a paper presented in September 1970 at the New York E.O.S.D. Conference by the two authors named.

Solid aluminium electrolytic capacitors, 121-series

B. Goudswaard
Philips Eindhoven

621.319.45

The solid aluminium capacitor is examined in detail, and its reliability is shown to be 100 times better than that of solid tantalum capacitors.

INTRODUCTION

Requirements specified by the users of electronic components have grown more and more stringent in recent years. For example, military and professional applications now require temperature ranges of −55°C to +125°C and higher and, in these temperature ranges, any changes from specified parameters are required to be as small as possible. Furthermore, high levels of reliability and long life are essential.

Development of the electrolytic capacitor has brought about many improvements in existing types, but a significant achievement has been the development and production of the new solid electrolyte aluminium foil capacitor. This article compares the new capacitor with the existing solid tantalum and liquid electrolyte ('wet') types and shows its several merits.

An outstanding feature of the solid aluminium capacitor is that both the high cost of a solid tantalum capacitor and the electrolyte losses (through evaporation during life, especially at high temperatures) of a wet aluminium capacitor have been avoided. Another point of great importance is the fact that the solid aluminium capacitor is about 100 times more reliable than the solid tantalum capacitor.

DEVELOPMENT BACKGROUND

Solid electrolyte tantalum capacitors have been on the market for several years. They are well suited to wide temperature ranges.

Instead of a liquid electrolyte, they use a semiconducting solid material, manganese dioxide, which is obtained by pyrolytic treatment of manganese nitrate. Manganese dioxide has the following advantages over liquid electrolytes:

1) changes in such parameters as capacitance and dissipation factor are much less because the specific resistance of manganese dioxide (hence the temperature coefficient) is much lower than that of liquid electrolytes;
2) the solid electrolyte cannot evaporate and does not change in composition during use, thus ensuring stability during high temperature operation and implying a long life.

However, tantalum capacitors with solid manganese dioxide electrolyte have some disadvantages. Tantalum is an expensive material. The failure rate of these capacitors is not especially good (10×10^{-6}/h); one of the reasons for this could be that solid tantalum capacitors do not possess the self-healing ability of the wet aluminium types. Self-healing is a decided advantage of the wet type of electrolytic capacitor.

Liquid electrolyte aluminium foil capacitors are much cheaper than tantalum capacitors. Therefore great efforts were made to extend their temperature range to give them a wider application. Extending the temperature range meant that new low specific resistance electrolytes and greatly improved case seals were required. However, this type of capacitor still does not meet the exacting standards of some professional applications.

It seemed natural to combine the qualities of a solid electrolyte such as manganese dioxide with the cost advantage of aluminium foil, so development of the solid electrolyte aluminium foil capacitor led to the 121 series of solid aluminium capacitors, outlined in Table 1 and Fig. 1.

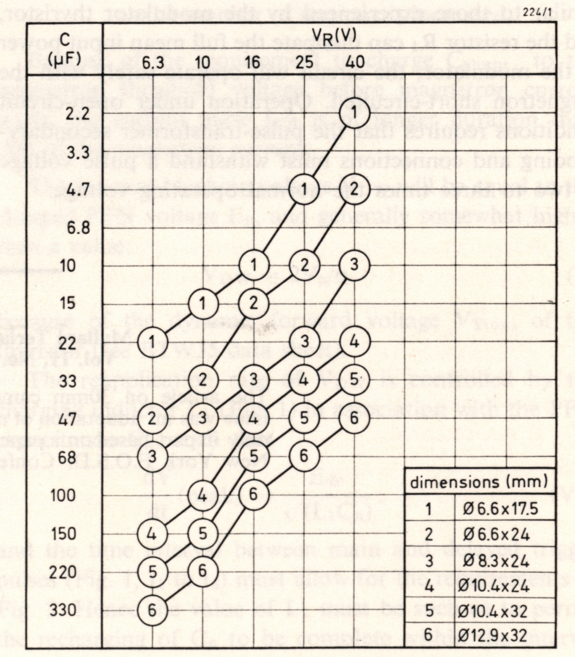

Fig. 1—121-series

TABLE 1

121-series data summary

Capacitance range:	2·2μF to 330μF (E6-series to I.E.C. 63)
Tolerance on capacitance:	±20%
Rated voltage (V_R) range:	6·3V to 40V
Temperature range:	−55°C to +85°C (rated voltage) −55°C to +125°C (derated voltage)
Test categories: (I.E.C. 68)	55/085/56 55/125/56

Compared with liquid electrolyte aluminium capacitors, they have the advantages of longer life and improved electrical parameter stability with temperature change; reverse voltages can be applied, and no reforming is necessary even after the most extensive shelf life.

Compared with solid tantalum capacitors, they have the advantages of greater reliability and higher ripple current rating; they have no discharge current limitation, and reverse voltages can be applied.

Their disadvantages are a smaller CV product per unit volume, and higher dissipation factor and leakage current.

APPLICATIONS

The most common functions of electrolytic capacitors are:

Decoupling. The capacitor presents a low impedance to alternating current between two amplifier stages, preventing undesirable signal voltages.

Bypassing. The capacitor offers a low impedance to the alternating current applied across the grid and cathode of an amplifying valve, thus keeping the cathode voltage low.

Coupling. The capacitor passes alternating current and blocks direct current between amplifying stages.

Smoothing. The capacitor reduces the ripple voltage of a power supply.

Solid aluminium capacitors may be used in all these functions and particularly where long life, great reliability, and high stability are essential and where high working temperatures are encountered.

CONSTRUCTION

Construction of the solid electrolyte aluminium capacitor is similar to that of the liquid electrolyte type. Three main differences exist:

1) A semi-conducting solid (manganese dioxide) is used as the electrolyte in place of a liquid.
2) The medium used to 'carry' the solid electrolyte is glass fibre, in place of the paper used in the liquid electrolyte type. Glass fibre is necessary to withstand the heat generated during pyrolysis.
3) The solid electrolyte capacitor is housed in a metal case which is sealed by a ceramic disc. Hermetic sealing is unnecessary as the capacitive element is impregnated with a material which enables it to withstand the most severe humidity tests. The sole purpose of the metal case is to give the capacitor mechanical strength.

PERFORMANCE CHARACTERISTICS

CV product

The CV product of the solid aluminium capacitor progresses from 150μFV to 2200μFV at 10V in six case sizes. This CV product range is about the same as that of the solid tantalum capacitor; however, the CV product per unit volume of the solid aluminium capacitor is only about one quarter of that of the solid tantalum type. Factors which contribute to this difference are:

1) *Dielectric constant*. The dielectric constant of tantalum pentoxide is much higher than that of aluminium oxide: the figures are 24 and 8 respectively.
2) *Construction*. Solid (and liquid) aluminium capacitors use etched aluminium foil wound as a 'cell' made up of two foils (anode and cathode) which are separated by a spacer containing the solid manganese dioxide (or liquid) electrolyte. Thus the cell is essentially two capacitors in series. A porous slug of sintered tantalum powder makes up the anode of the solid tantalum capacitor, and its cathode is formed by a very thin layer of graphite beneath a (solderable) silver layer. This gives the solid tantalum capacitor a greater surface area (per unit volume) than the solid aluminium capacitor, but the types of surface make it difficult to calculate the exact value of this factor.
3) *Forming voltage*. The disadvantages (for the solid aluminium capacitor) of (1) and (2) above are somewhat offset when the forming voltages required by solid aluminium and solid tantalum capacitors are taken into consideration. During formation of the oxide layers it is possible that impurities and variations in field strength may create weak spots. To prevent breakdown failures it is necessary to form the anode at a higher voltage than the rated voltage. The ratio between the forming voltage and rated voltage is about 2 : 1 for solid (and liquid) aluminium capacitors and can vary between 3 : 1 and 6 : 1 for solid tantalum (because the dielectric does not self-heal during service life). The lower this ratio, the higher the CV product per unit volume.

Comparison of solid and liquid aluminium capacitors shows that the CV product of the solid type is about half that of the liquid type. The reason for this is that the pores of the etched aluminium foil are only partly filled with manganese dioxide. Further pyrolysis will improve the filling grade but it also increases the leakage current, therefore an optimum filling grade has been determined. It is this which limits the maximum rated voltage (40V at present, but further development will extend this limit).

Capacitance

Values of capacitance, with a tolerance of ±20%, range from 2·2μF to 330μF (in E6 series). Fig. 2 shows the effect of temperature on capacitance over the working temperature range of −55°C to +125°C. A comparison of the changes in capacitance between the top and bottom of the working temperature range, and room temperature, for three types of electrolytic capacitor, is given in Table 2.

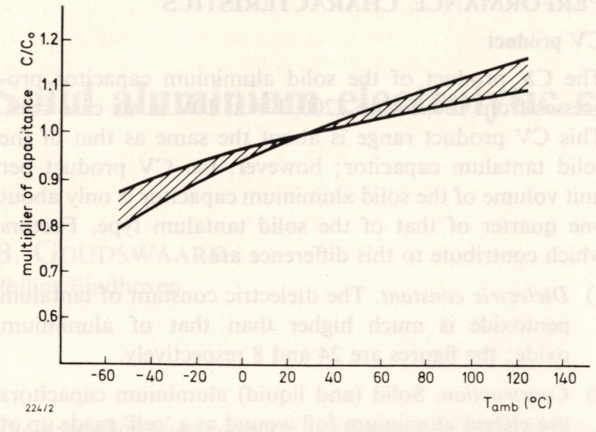

Fig. 2—Typical change of capacitance with ambient temperature. C_o = capacitance at 25°C, 100Hz

TABLE 2

Comparison of changes in capacitance at extreme working temperatures.

Type of capacitor	Capacitance change from 25°C value 125°C (%)	−55°C (%)
Wet Al	+15 to +20	−20 to −30
Solid Al	+10 to +15	−10 to −20
Solid Ta	+5 to +10	−5 to −10

Capacitance, with particular reference to electrolytic capacitors, is a collective term by which it is understood that the total capacitance is distributed over the surface of the pores in the etched aluminium foil or sintered tantalum slug. The dielectric layer is connected to the cathode by the electrolyte in the pores and this connection takes the form of distributed resistance. The bulk of the electrolyte completes electrical contact between dielectric and cathode. In electrolytic capacitors, the change in capacitance with temperature is mainly determined by the distributed resistance in the pores.

As the temperature decreases, the resistance of the electrolyte increases and will eventually exceed the capacitive reactance. Contact between the electrolyte and the oxide layer in the deepest pores is therefore of such high resistance that these areas no longer contribute to the total capacitance. As temperature increases, the reverse process occurs. The effect becomes more pronounced as the temperature coefficient of the electrolyte increases, as the depth of the pores increases, and as the diameter of the pores decreases.

Table 2 shows that the change in capacitance with temperature is greater for solid aluminium capacitors than for solid tantalum. The reason for this difference is that the pores in the surface of the highly etched aluminium foil are smaller than the pores in the sintered tantalum slug. Having smaller pores means that, before pyrolysis, manganese nitrate cannot penetrate into the pores as efficiently as in solid tantalum. Therefore after pyrolysis the pores of the etched aluminium are only partly filled with manganese dioxide.

Changes in the capacitance of solid aluminium capacitors are smaller than those of wet aluminium capacitors. This is because the specific resistance of the various liquid electrolytes used is greater than the specific resistance of manganese dioxide. The temperature coefficient of the liquid electrolytes is also higher than that of the solid manganese dioxide.

Dissipation factor

Equivalent series resistance, R_s, plays an important part in calculating the dissipation factor of electrolytic capacitors. Factors which determine R_s are:

1) dielectric losses;
2) distributed electrolyte resistance in the pores;
3) bulk resistance between anode and cathode.

Dielectric losses are independent of the capacitance value. The contribution of the series resistance of the electrolyte towards dissipation factor decreases with decrease in capacitance (for the same case size), therefore there are lower losses in capacitors with the higher rated voltages.

Table 3 gives the dissipation factor for three types of electrolytic capacitor at 100Hz and 25°C. Comparing the figures for the solid aluminium and solid tantalum types shows that the solid aluminium capacitor has the higher losses.

TABLE 3

Comparison of dissipation factor

Type of capacitor	tanδ at 100Hz at 25°C	Multiplying factor from 25°C value of tanδ or ESR at 100Hz at −55°C
Wet Al	0·1 to 0·2	10 to 20 (depending on electrolyte)
Solid Al	0·08 to 0·15	2 to 3 (see Fig. 3)
Solid Ta	0·03 to 0·06	2 to 3

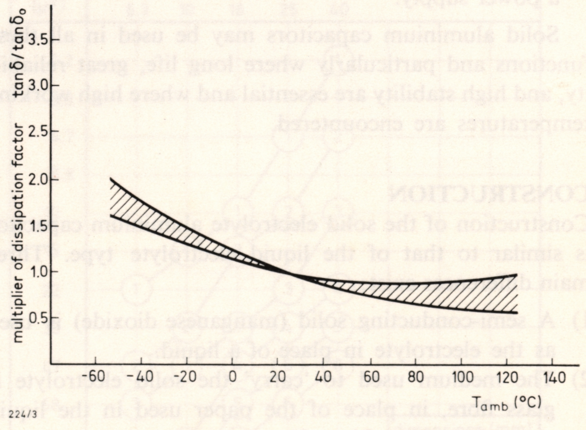

Fig. 3—Typical dissipation factor versus ambient temperature tan δ_o = dissipation factor at 25°C, 100Hz

These losses are the result of the lower filling grade of the smaller pores, and the higher dielectric losses caused by hydration of the oxide layer during the pyrolytic process. Lower filling grade and higher dielectric losses together make the dissipation factor of the solid aluminium capacitor slightly less than that of the wet type at room temperature. However, the degree to which the dissipation factor of solid aluminium capacitors depends on temperature, compares reasonably well with that of solid tantalum.

Impedance

Capacitance, series resistance, and self-inductance determine the impedance of an electrolytic capacitor. Figs. 4 and 5 show the impedances of various capacitors in the six case sizes as a function of frequency. Three frequency ranges can be distinguished:

1) *Less than 1kHz.* In this low frequency range, the influence of series resistance and self-inductance on impedance can be neglected.
2) *1kHz to 100kHz.* At higher frequencies impedance is influenced by the distributed series resistance of the pores. This pore effect causes the impedance curve to flatten with increase in frequency. As frequency increases, capacitive reactance becomes lower than the electrolyte resistance. The capacitance then decreases because the deepest pores no longer contribute to the total capacitance.
3) *Over 100kHz.* Impedance falls to a minimum at some high frequency. At this point, capacitive and inductive reactances are so low that the impedance is determined by the electrolyte resistance. At very high frequencies, self-inductance predominates and increases the impedance. Bifilar winding of the capacitor cell reduces the self-inductance of the solid aluminium capacitor to a minimum (20nH).

Graphs of impedance plotted against temperature, with frequency as a parameter, are shown in Figs. 6 to 11. The effect of electrolyte resistance on impedance at low temperature is far less for the solid aluminium capacitor than for wet types. Here the reason is the large difference in temperature coefficients of the electrolytes.

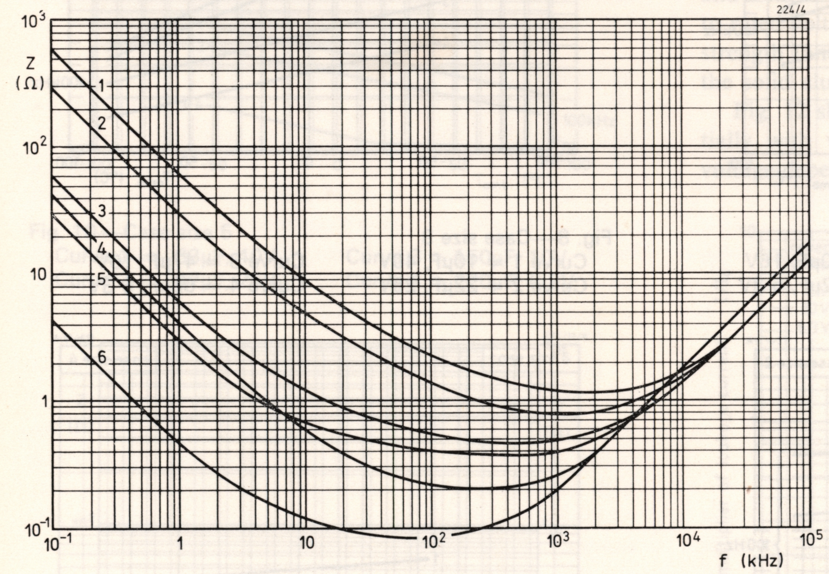

Fig. 4—Impedance versus frequency at 25°C
Curve 1 = 2·2μF, 40V
Curve 2 = 4·7μF, 40V
Curve 3 = 22μF, 6·3V
Curve 4 = 47μF, 40V
Curve 5 = 47μF, 6·3V
Curve 6 = 330μF, 6·3V.

Curves 1 and 3 = case size 1
Curves 2 and 5 = case size 2
Curves 4 and 6 = case size 6

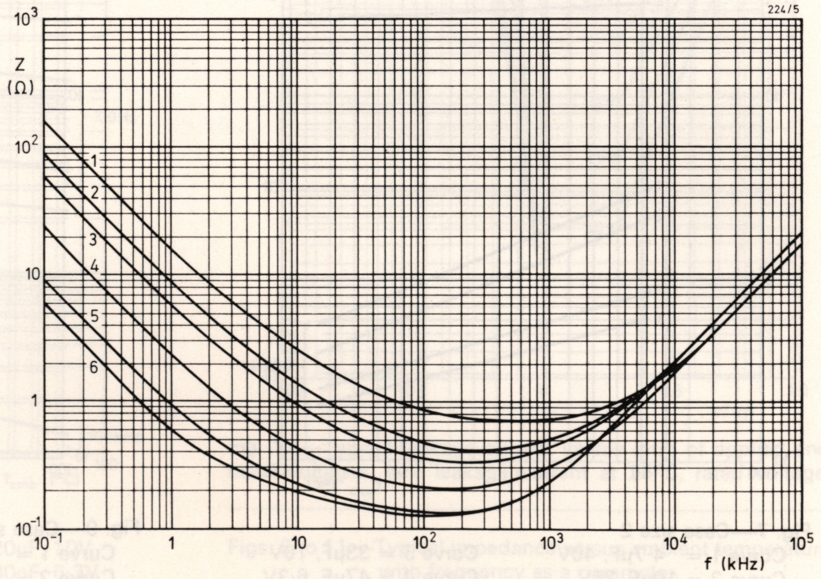

Fig. 5—Impedance versus frequency at 25°C
Curve 1 = 10μF, 40V
Curve 2 = 22μF, 40V
Curve 3 = 33μF, 40V
Curve 4 = 68μF, 6·3V
Curve 5 = 150μF, 6·3V
Curve 6 = 220μF, 6·3V.

Curves 1 and 4 = case size 3
Curves 2 and 5 = case size 4
Curves 3 and 6 = case size 5

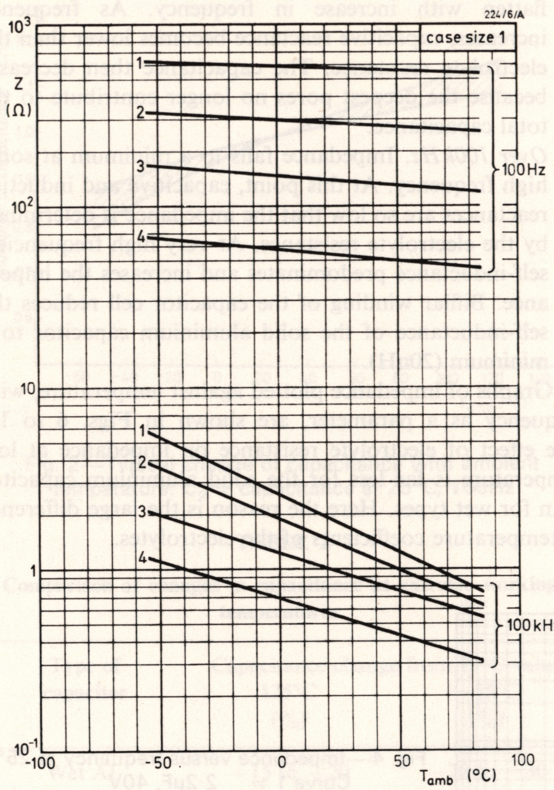

Fig. 6—Case size 1
Curve 1 = 2·2μF, 40V
Curve 2 = 4·7μF, 25V
Curve 3 = 10μF, 16V
Curve 4 = 22μF, 6·3V

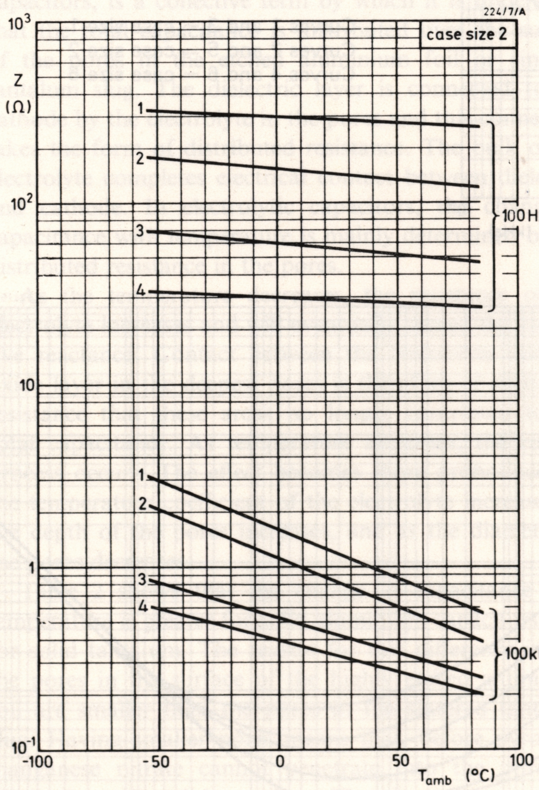

Fig. 7—Case size 2
Curve 1 = 4·7μF, 40V
Curve 2 = 10μF, 25V
Curve 3 = 33μF, 10V
Curve 4 = 47μF, 6·3V

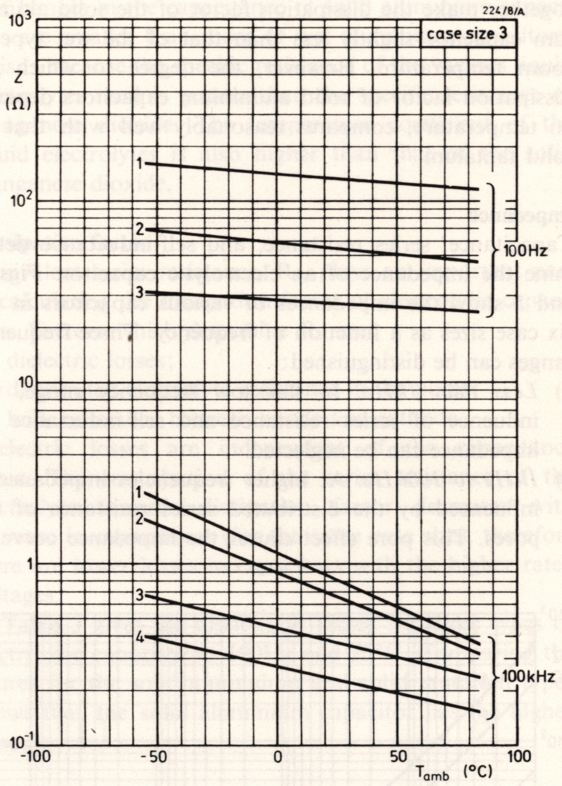

Fig. 8—Case size 3
Curve 1 = 10μF, 40V
Curve 2 = 22μF, 25V
Curve 3 = 47μF, 10V
Curve 4 = 68μF, 6·3V

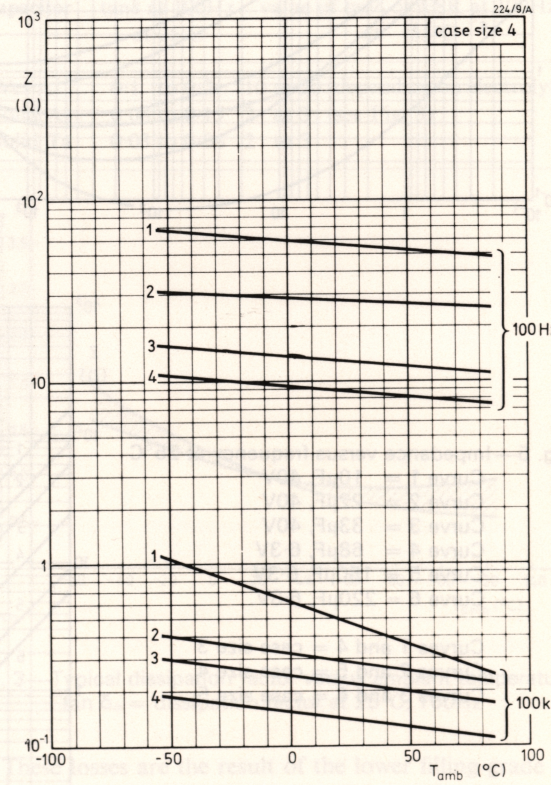

Fig. 9—Case size 4
Curve 1 = 22μF, 40V
Curve 2 = 47μF, 16V
Curve 3 = 100μF, 10V
Curve 4 = 150μF, 6·3V

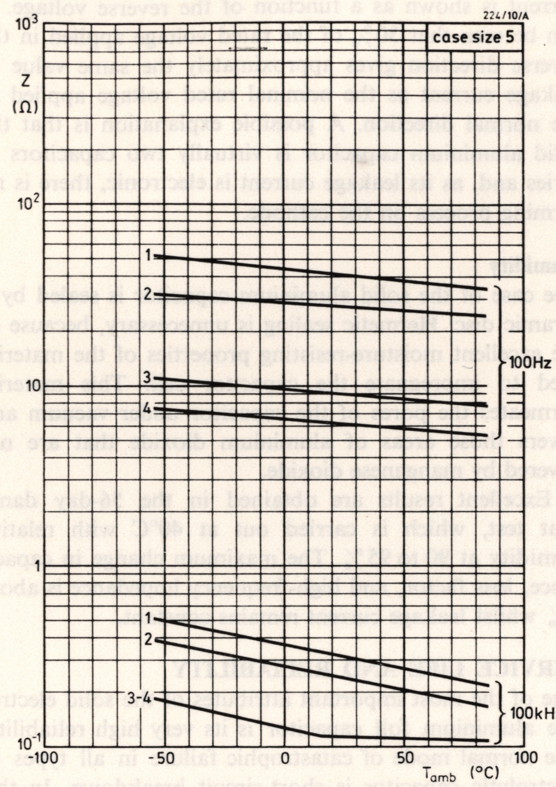

Fig. 10—Case size 5
Curve 1 = 33μF, 40V
Curve 2 = 47μF, 25V
Curve 3 = 150μF, 10V
Curve 4 = 220μF, 6·3V

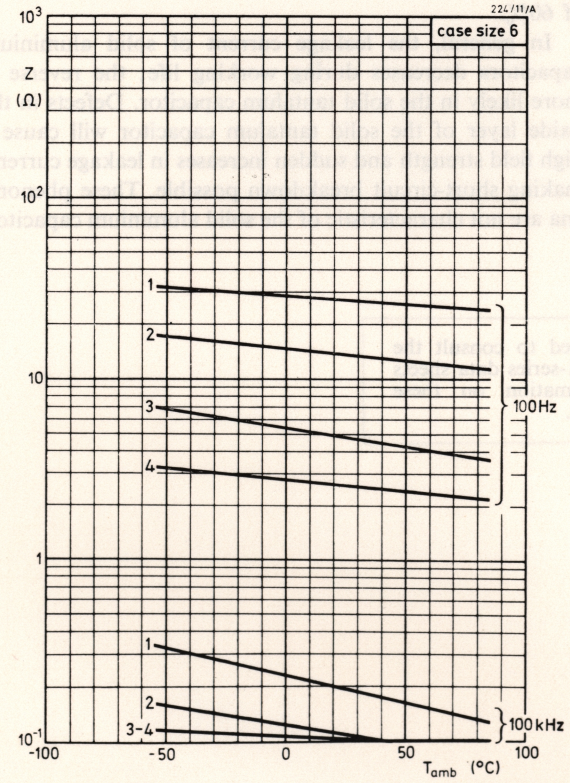

Fig. 11—Case size 6
Curve 1 = 47μF, 40V
Curve 2 = 100μF, 16V
Curve 3 = 220μF, 10V
Curve 4 = 330μF, 6·3V

Leakage current

The leakage current of a capacitor is determined by the charge on its electrodes and is proportional to capacitance and voltage, where

$$I = kCV$$

with I (the leakage current) measured in μA, C in μF, and V in volts. The factor k is determined by the field strength of the dielectric layer and is temperature-dependent. Table 4 gives the k values of three types of capacitor at different temperatures.

TABLE 4: k factors at different temperatures

Type of capacitor	k value at +25°C	k value at +85°C
Wet Al	0·005	0·15
Solid Al	0·1	0·7
Solid Ta	0·02	0·2

The large difference in k value between solid aluminium and solid tantalum is due to the difference in their forming-to-rated voltage ratios. At the same rated voltage, the field strength (and consequently leakage current) is higher for the solid aluminium capacitor than for solid tantalum.

Fig. 12 shows that leakage current increases exponentially with voltage and that the slope of the curve is voltage-dependent.

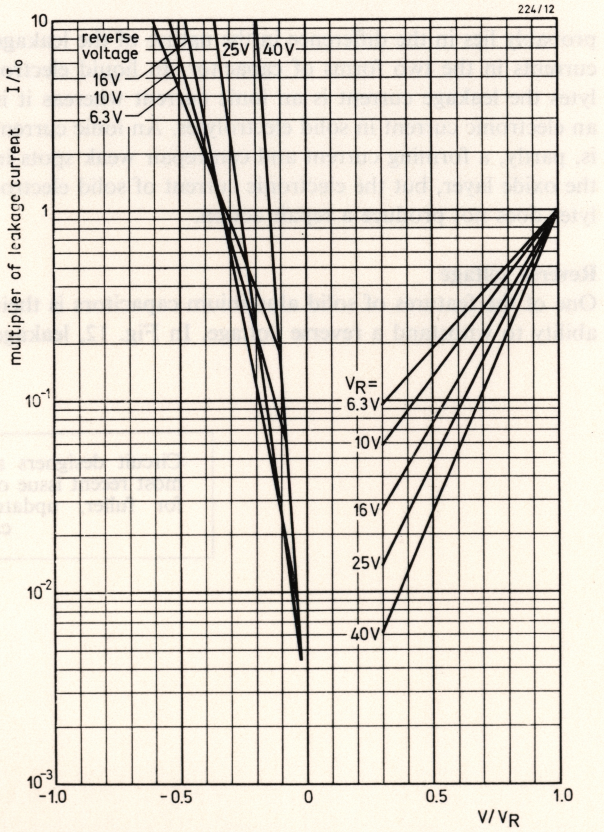

Fig. 12—Typical leakage current versus ratio of applied and rated voltages. I₀ = leakage current at 25°C, rated voltage.

Figs. 6 to 11—Typical impedance versus ambient temperature with frequency as a parameter.

The effect of temperature on leakage current in solid aluminium capacitors is shown in Fig. 13: the graph for solid tantalum capacitors is similar.

Liquid electrolyte capacitors have a considerably lower leakage current than solid types. The reason for this probably lies in the difference in the nature of the leakage currents in the two forms of capacitor. In liquid electrolytes the leakage current is an ionic current whereas it is an electronic current in solid electrolytes. An ionic current is, partly, a forming current and can repair weak spots in the oxide layer, but the electronic current of solid electrolytes does not produce a repair action.

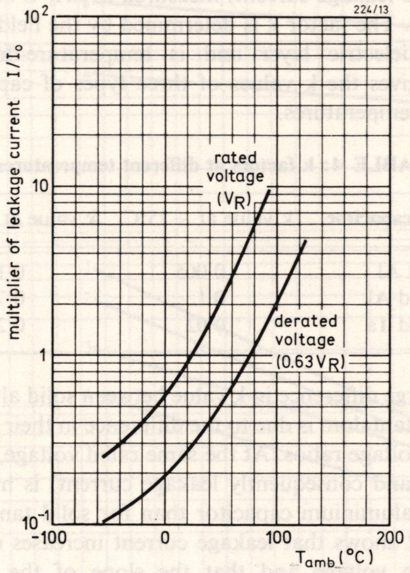

Fig. 13—Typical leakage current versus ambient temperature I_o = leakage current at 25°C, rated voltage

Reverse voltage

One of the features of solid aluminium capacitors is their ability to withstand a reverse voltage. In Fig. 12, leakage current is shown as a function of the reverse voltage. It can be seen that 30% of the rated voltage applied in the reverse direction gives approximately the same value of leakage current as the nominal rated voltage applied in the normal direction. A possible explanation is that the solid aluminium capacitor is virtually two capacitors in series and, as its leakage current is electronic, there is no forming process on the cathode.

Humidity

The case of the solid aluminium capacitor is sealed by a ceramic disc. Hermetic sealing is unnecessary, because of the excellent moisture-resisting properties of the material used to impregnate the capacitor cell. This material permeates the pores of the capacitor under vacuum and covers those areas of aluminium dioxide that are not covered by manganese dioxide.

Excellent results are obtained in the 56-day damp heat test, which is carried out at 40°C with relative humidity at 90 to 95%. The maximum change in capacitance, loss factor, and high-frequency impedance is about 4% whilst leakage current remains constant.

SERVICE LIFE AND RELIABILITY

One of the most important attributes of the solid electrolyte aluminium foil capacitor is its very high reliability. The normal mode of catastrophic failure in all types of electrolytic capacitor is short-circuit breakdown. In this respect the solid aluminium capacitor is about 100 times better than the solid tantalum capacitor. Failure rate in solid aluminium capacitors, based on more than 25×10^6 component hours, is $0{\cdot}11 \times 10^{-6}$/h with a confidence level of 60%.

In general, the leakage current of solid aluminium capacitors decreases during working life; the reverse is more likely in the solid tantalum capacitor. Defects in the oxide layer of the solid tantalum capacitor will cause a high field strength and sudden increases in leakage current, making short-circuit breakdown possible. These phenomena are not characteristic of the solid aluminium capacitor.

Circuit designers are advised to consult the most recent issue of the 121-series data sheets for fuller, updated information on these capacitors.